Article

Cell Reports

A c-Myc/miR17-92/Pten Axis Controls PI3K-Mediated Positive and Negative Selection in B Cell Development and Reconstitutes CD19 Deficiency

Graphical Abstract

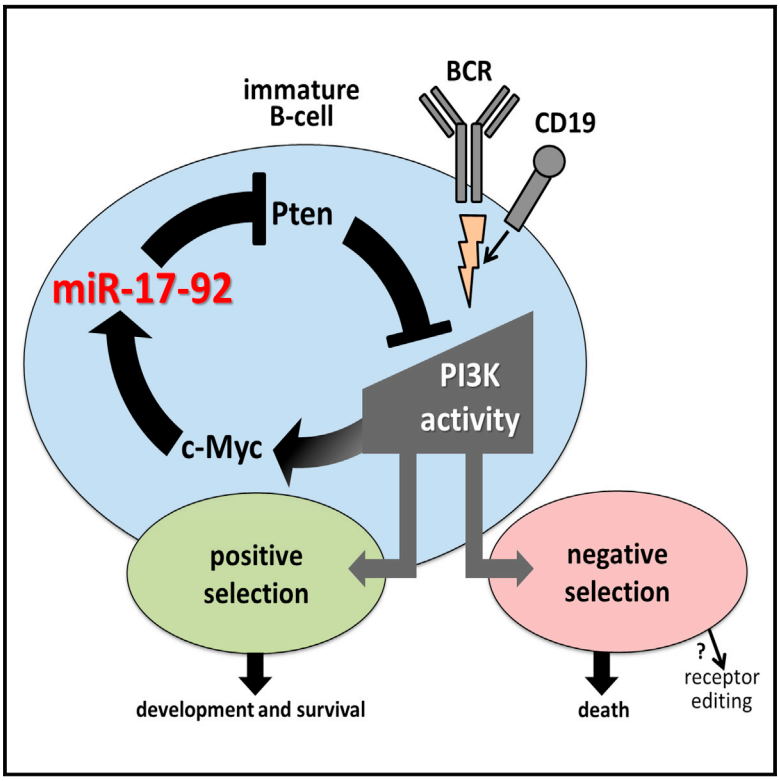

Authors

David Benhamou, Verena Labi, Rostislav Novak, ..., Shai S. Shen-Orr, Klaus Rajewsky, Doron Melamed

Correspondence

melamedd@tx.technion.ac.il

In Brief

Benhamou et al. show that phosphoinositide 3-kinase directly activates an autostimulatory c-Myc/miR17-92/Pten axis to control itself for B cell-fate decisions during positive and negative selection.

Highlights

- PI3K controls itself through post-transcriptional regulation of Pten
- This regulation is facilitated via c-Myc/miR17-92/Pten autostimulatory axis
- c-Myc/miR17-92/Pten regulates PI3K-mediated B cell positive and negative selection
- Overexpression of miR17-92 reconstitutes B cell development in CD19-deficient mice

Benhamou et al., 2016, Cell Reports *16*, 419–431
July 12, 2016
http://dx.doi.org/10.1016/j.celrep.2016.05.084

CellPress

Cell Reports
Article

A c-Myc/miR17-92/Pten Axis Controls PI3K-Mediated Positive and Negative Selection in B Cell Development and Reconstitutes CD19 Deficiency

David Benhamou,[1,4] Verena Labi,[2,4] Rostislav Novak,[1] Isabelle Dai,[1] Shani Shafir-Alon,[1] Ariel Weiss,[1] Renaud Gaujoux,[1] Rüdiger Arnold,[3] Shai S. Shen-Orr,[1] Klaus Rajewsky,[2] and Doron Melamed[1,*]
[1]Department of Immunology, Faculty of Medicine, Technion – Israel Institute of Technology, Haifa 31096, Israel
[2]Max Delbrück Center for Molecular Medicine, 13125 Berlin, Germany
[3]Tumor Immunology Program, German Cancer Research Center (DKFZ), 69120 Heidelberg, Germany
[4]Co-first author
*Correspondence: melamedd@tx.technion.ac.il
http://dx.doi.org/10.1016/j.celrep.2016.05.084

SUMMARY

PI3K activity determines positive and negative selection of B cells, a key process for immune tolerance and B cell maturation. Activation of PI3K is balanced by phosphatase and tensin homolog (Pten), the PI3K's main antagonistic phosphatase. Yet, the extent of feedback regulation between PI3K activity and Pten expression during B cell development is unclear. Here, we show that PI3K control of this process is achieved post-transcriptionally by an axis composed of a transcription factor (c-Myc), a microRNA (miR17-92), and Pten. Enhancing activation of this axis through overexpression of miR17-92 reconstitutes the impaired PI3K activity for positive selection in CD19-deficient B cells and restores most of the B cell developmental impairments that are evident in CD19-deficient mice. Using a genetic approach of deletion and complementation, we show that the c-Myc/miR17-92/Pten axis critically controls PI3K activity and the sensitivity of immature B cells to negative selection imposed by activation-induced cell death.

INTRODUCTION

Fate decisions of developing B cells critically depend on signals that are generated by the B cell antigen receptor (BCR). Immature and transitional B cells encountering self-antigens undergo negative selection by receptor editing or are eliminated by apoptosis (clonal deletion), whereas appropriate ligand-independent basal signals are thought to promote development and maturation of cells expressing innocuous receptors in a process referred to as positive selection (Monroe, 2006; Rowland et al., 2013). BCR-mediated negative selection has been demonstrated in mutant and normal mice and was found to depend on developmental stage or site of self-antigen encounter (Edry and Melamed, 2004; Monroe, 2006; von Boehmer and Melchers, 2010). The deletion of these cells is facilitated by a mechanism called activation-induced cell death (AICD) (Donjerković and Scott, 2000; Eeva and Pelkonen, 2004). Impaired positive selection has been shown in mice deficient in BCR signaling regulatory co-receptors such as CD45 and CD19, as reflected by a significant reduction in numbers of B cell in the periphery (Cyster et al., 1996; Rickert et al., 1995). Crossing of CD45-and-CD19-deficient mice with immunoglobulin transgenic mice to express an innocuous BCR suggests that this positive selection is mediated by ligand-independent signals (Cyster et al., 1996; Shivtiel et al., 2002). Inappropriate basal signals impose a developmental block of immature B cells and ongoing rearrangements (Diamant et al., 2005; Shivtiel et al., 2002; Verkoczy et al., 2007). However, whereas in mature B cells the dependence on tonic BCR activity for survival has been demonstrated (Srinivasan et al., 2009), the nature of ligand-independent signals for B cell positive selection is not completely understood.

The phosphoinositide 3-kinase (PI3K) pathway has emerged as a critical determinant for B cell development and survival (Herzog et al., 2008; Okkenhaug and Vanhaesebroeck, 2003; Srinivasan et al., 2009; Werner et al., 2010) and has been found to be involved in both positive (Diamant et al., 2005; Monroe, 2006; Shivtiel et al., 2002; Tze et al., 2005; Verkoczy et al., 2007) and negative (Cheng et al., 2009; Clayton et al., 2002; Pogue et al., 2000) selection. CD19 is the main contributor for PI3K activity in B lineage cells as it directly associates with PI3K upon phosphorylation by Src-family kinases (Tuveson et al., 1993). Inappropriate PI3K activity is often associated with pathological manifestations with impaired signaling leading to immunodeficiency, whereas unrestrained signaling promotes autoimmunity and leukemia (reviewed in Okkenhaug and Vanhaesebroeck, 2003). This paradigm is best exemplified in mice where CD19 expression is altered: CD19-deficient mice have severe defects in B cell development, activation, and differentiation (Diamant et al., 2005; Engel et al., 1995; Rickert et al., 1995; Shivtiel et al., 2002), whereas mice transgenic for human CD19 develop autoimmunity (Engel et al., 1995). More recently, CD19 was found to be a major BCR-independent regulator of c-Myc levels in B cell neoplasms by activating the PI3K/Akt/GSK3 axis to promote B cell transformation and lymphoma progression (Chung et al., 2012; Poe et al., 2012). Hence, appropriate tuning of PI3K activity is critical for life and death decisions during positive and negative selection of B cells.

Whereas CD19 is the major activator of PI3K in B lineage cells, the phosphatase and tensin homolog (Pten) has the major role of balancing PI3K activity by converting PIP3 to PIP2 (Suzuki et al., 2008). Pten is expressed in B lineage cells and has been shown to play a role in B cell differentiation (Alkhatib et al., 2012; Anzelon et al., 2003; Suzuki et al., 2003). Moreover, Pten heterozygosity is sufficient to result in significantly enhanced PI3K activity (Suzuki et al., 1998), and ablating both Pten alleles reconstitutes B1 and marginal zone (MZ) B cell development in CD19$^{-/-}$ (CD19KO) mice (Anzelon et al., 2003). However, the extent of feedback regulation between PI3K signaling and Pten expression during B cell development is unclear. Several studies have shown that some PI3K components inhibit Pten function (reviewed in Carracedo and Pandolfi, 2008) and provided suggestive evidence for the existence of such a reciprocal regulatory mechanism. More recently, a genomic screening of Burkitt's lymphoma cells suggested that the overexpression of c-Myc, which is the defining oncogene of this cancer, and its target microRNA17HG inhibit Pten and augment PI3K activity, resulting in increased tumorogenicity (Schmitz et al., 2012). However, the relevance of this to normal cells, where the expression of c-Myc and its target genes is tightly regulated, is unclear.

Here, we explored the role of microRNAs (miRNAs) as potential mediators by which the PI3K pathway controls Pten expression in developing B cells. Using CD19KO mice that conditionally overexpress miR17-92 in the B lineage, we show an axis composed of a transcription factor (c-Myc), a miRNA cluster (miR17-92) and a signaling molecule (Pten), which is directly activated by PI3K to physiologically control expression of Pten during B cell development. We found that the c-Myc/miR17-92/Pten axis is critical for balancing PI3K activity in its control of B cell-fate decisions for positive and negative selection. Furthermore, we found that overexpression of miR17-92 effectively compensated for the impaired PI3K activity in CD19-deficient B cells thereby reconstituting the majority of B cell developmental impairments that are evident in CD19KO mice.

RESULTS

Ablation of Dicer Impairs PI3K Signaling and Stimulates Apoptosis of Transitional B Cell, Whereas Pten Heterozygosity Restores PI3K Activity to Promote Survival

PI3K activity is necessary to promote positive selection of immature and transitional B cells (Diamant et al., 2005; Monroe, 2006; Shivtiel et al., 2002; Tze et al., 2005; Verkoczy et al., 2007). Since miRNAs have been shown in a variety of systems to be critical regulators of developmental checkpoints, we studied whether microRNAs regulate life and death decisions at this developmental checkpoint. To address this globally, we decided to establish an inducible system to generate Dicer-ablated transitional B cells in vivo, since conditional deletion of Dicer in proB cells blocks Pro-to-preB cell development and stimulates preB cell apoptosis (Koralov et al., 2008). In these experiments, we used mice transgenic for human CD20 (hCD20), where B cells are eliminated upon administration of mouse anti-human CD20 antibodies (Ahuja et al., 2007), to set up a depletion-autoreconstitution mouse model where most of the splenic B cells are at the transitional stage (Figure S1). We crossed these strains to generate hCD20Tg/Mx-cre/Dicer$^{fl/fl}$ mice, where we induced ablation of Dicer in transitional B cells upon administration of poly(I)(C). Deletion of Dicer in B cells upon this treatment was confirmed by the absence of miRNAs (Figure S2). We found that the dicer ablated mice had a dramatic loss of >70% of transitional B cells in the spleen (from 26% in hCD20 to 7% in hCD20Tg/Mx-cre/Dicer$^{fl/fl}$ mice; Figures 1A and 1C), and Annexin V staining revealed that this loss is caused by apoptosis (Figures 1B and 1C). Intracellular flow cytometry analysis revealed that in Dicer-ablated transitional B cells PI3K activity is impaired, as reflected by the profoundly reduced level of Akt phosphorylation (Figure 1D; MFI = 585 relative to control MFI = 707). Hence, we concluded that the global reduction in miRNAs impairs PI3K signaling in transitional B cells and stimulates apoptosis of these cells.

Next, we tested how the global reduction of miRNAs can suppress PI3K activity. One possible mechanism by which this suppression may be achieved is through enhanced expression of the tumor suppressor Pten. Indeed, analysis of splenic B cells from Dicer-ablated mice revealed that expression of Pten is significantly elevated (Figure 1E). To confirm the physiological relevance of this mechanism, we tested whether reducing expression of Pten can reconstitute PI3K activity to rescue Dicer-ablated transitional B cells. We decided to use an inducible genetic approach by ablating only one Pten allele in mice, since Pten heterozygosity is sufficient to result in significantly enhanced PI3K activity (Suzuki et al., 1998). To achieve this, we generated hCD20Tg/Mx-cre/Dicer$^{fl/fl}$/Pten$^{fl/+}$ mice and co-ablated both Dicer alleles and one of the Pten alleles in transitional cells. This experimental maneuver effectively reconstituted tonic PI3K activity (measured by Akt phosphorylation; Figure 1D; MFI = 901 relative to control MFI = 707 and Dicer ablated MFI = 585) and promoted survival of transitional B cells (revealed by total B cells numbers and %Annexin V staining; Figures 1A–1C). Hence, we concluded that a regulatory network exists between PI3K and Pten whose role is to tune PI3K activity for positive selection, and that this network is mediated post-transcriptionally by miRNAs. In the next set of experiments, we attempted to identify this network.

The c-Myc/miR17-92/Pten Axis Regulates Pten Expression to Balance PI3K Activity in B Lineage Cells

A major mechanism by which PI3K promotes survival is by increasing the expression of c-Myc transcription factor (Sears, 2004). Thus, we next tested whether c-Myc regulates the expression of Pten, to enhance PI3K activity and to promote survival, in a miRNA-mediated mechanism. One possible mechanism by which c-Myc can exert this regulation is via miR17-92, as the miR17-92 locus is a direct target of c-Myc (O'Donnell et al., 2005), and the miR17-92 cluster negatively controls expression of Pten (Xiao et al., 2008). Hence, we hypothesized that a c-Myc/miR17-92/Pten autostimulatory loop exists and enhances activation of the PI3K pathway. Accordingly (as illustrated in Figure 2A), a PI3K-mediated increase in c-Myc stimulates expression of miR17-92, should, in turn, lead to degradation of Pten mRNA (and perhaps inhibition of Pten translation),

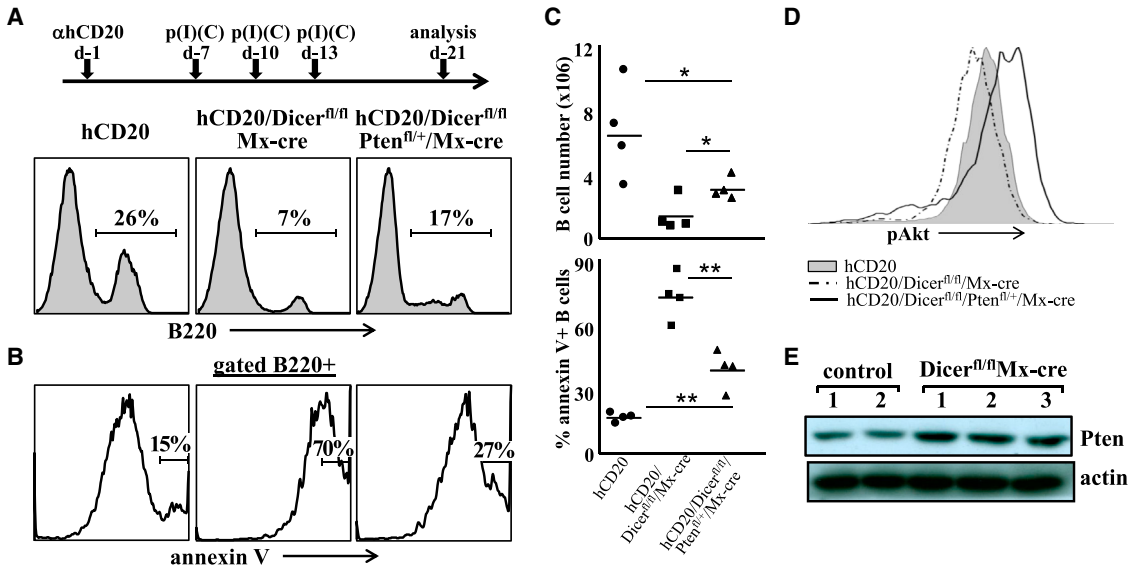

Figure 1. Ablation of One Pten Allele Promotes Survival of Dicer-Deleted Transitional B Cells

Mice with the indicated genotypes were injected with mouse anti-hCD20 to deplete B cells (depletion-autoreconstitution model for generation of transitional B cells in the spleen, see Supplemental Information). On days 7, 10, and 13, mice were injected with poly (I)(C) (400 μg/mouse/injection), and splenic B cells were analyzed on day 21.

(A) Time scheme of the experiment (top), and a representative fluorescence-activated cell sorting (FACS) analysis of percentage of B cells among total splenocytes ($B220^+$, bottom).

(B) Annexin V staining of splenic B cells (gated on $B220^+$).

(C) Graphs depict total cell numbers of splenic B cells shown in (A) (top) and percentage of annexin V^+ B cells shown in (B) (bottom) for individual mice and group mean (n = 4). Significance shown is *$p < 0.05$; **$p < 0.001$.

(D) Flow cytometry analysis for baseline pAkt (S473, gated on $B220^+$ splenic cells).

(E) Splenic B cells from control and Dicer-ablated mice [treated with poly(I)(C)] were lysed and expression of the indicated proteins was determined by western blotting. Shown are representative results for two control and three Dicer-ablated mice (from n = 4 for each group).

thus increasing activation of the PI3K pathway. Indeed, these regulatory connections were supported by a Gene Set Enrichment Analysis (GSEA) which highlighted the enrichment (i.e., change in rank) of shared Myc miR-17-92 and mirR-17-92 only targets between gene expression profiles of CD19 high and low B cells (Figure 2B, top and bottom panels, respectively; see Supplemental Experimental Procedures; NES = 1.47, $p < 0.02$, and NES = 1.35, $p < 0.07$ for shared miR-172 and Myc and miR-172 only targets, respectively).

To validate the relevance of a potential c-Myc/miR17-92/Pten loop in B cells, we used splenic B cells from CD19KO mice, where activation of the PI3K pathway is impaired (Buhl et al., 1997; Otero et al., 2001) (see also Figure S5). Consequential to the dampened PI3K activity, expression of c-Myc in CD19KO B cells is significantly reduced relative to wild-type (WT) B cells (Figure 2C; Chung et al., 2012). In agreement with our hypothesis and the low levels of c-Myc, we found in CD19KO B cells significantly reduced expression of miR19b (miRNA of the miR17-92 cluster that binds to the 3′ UTR of Pten [Xiao et al., 2008]), whereas Pten mRNA and protein expression were significantly increased, relative to WT B cells (Figures 2C and 2D).

To link the altered miR19b and Pten expression in CD19KO B cells to the reduced expression of c-Myc in these cells, we used GSK3 inhibitors that prevent degradation of c-Myc. We found that elevating c-Myc in CD19KO B cells (Figure 2C, right lane) increased the expression of miR19b and repressed the expression of Pten protein and mRNA to levels not different than those found in WT B cells (Figures 2C and 2D). To confirm these findings, we performed the reciprocal experiment where we treated WT B cells with anti-sense c-Myc oligonucleotides to reduce its expression (Leider and Melamed, 2003) (see also Figure S7). As shown in Figure 2E, this resulted in a significantly reduced expression of miR19b and increased levels of Pten. Hence, we concluded that an autostimulatory axis containing the transcription factor c-Myc, miR17-92, and the signaling molecule Pten regulates the PI3K pathway and that this loop is impaired in CD19KO B cells (Figure 2E).

Overexpression of miR17-92 Restores PI3K Signaling and Partially Rescues B Cell Development and Positive Selection in CD19KO Mice

Since PI3K signaling is critical for B cell development (Clayton et al., 2002), our findings suggested an important role of the c-Myc/miR17-92/Pten axis in the regulation of this process. This hypothesis was supported by an earlier study showing that ablation of Pten rescues development of B1 and marginal zone (MZ) B cells in CD19KO mice (Anzelon et al., 2003), where PI3K activation and positive selection are impaired (Diamant et al., 2005). Based on this and our results, we postulated that overexpression of miR17-92 would reconstitute PI3K activity to

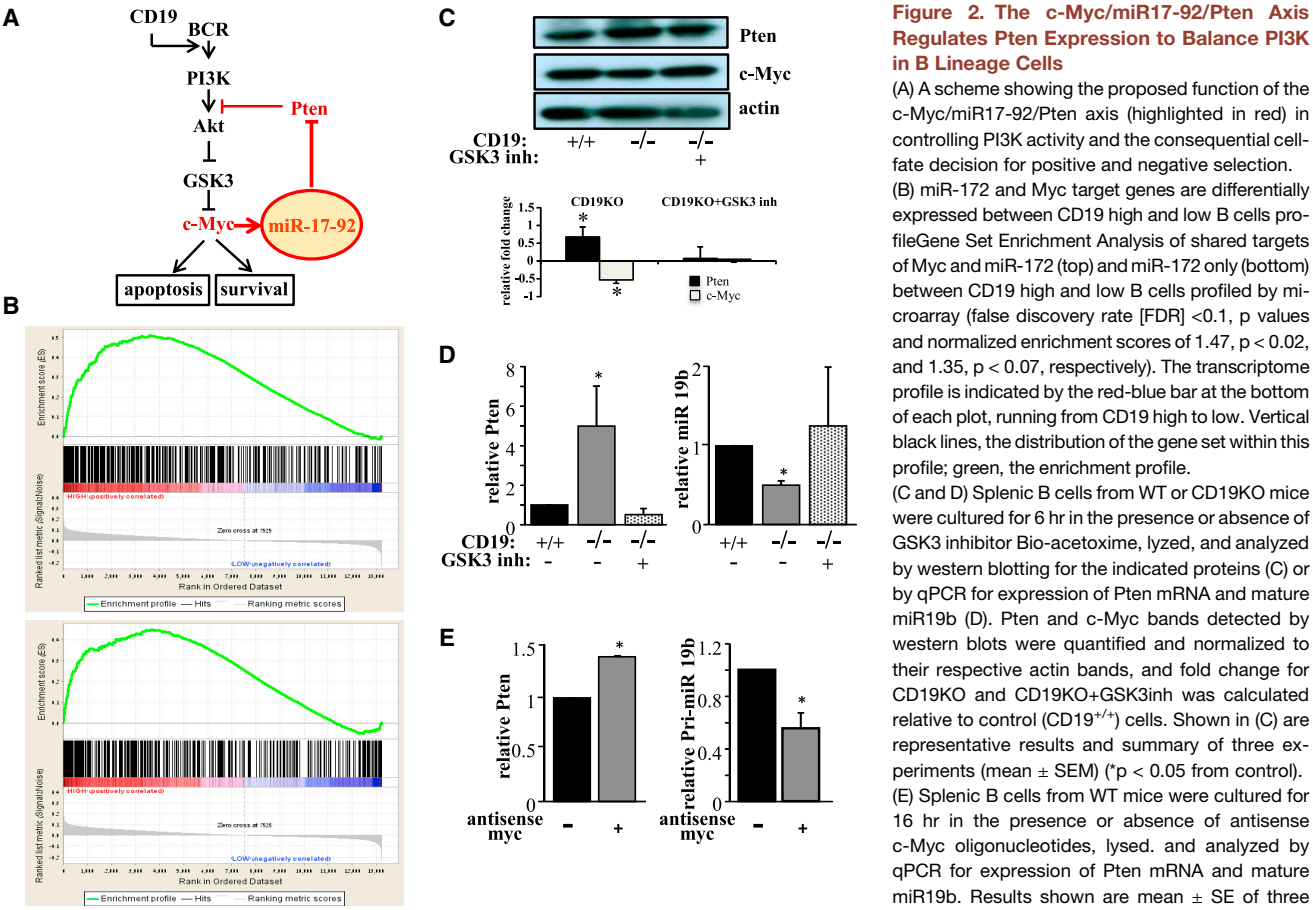

Figure 2. The c-Myc/miR17-92/Pten Axis Regulates Pten Expression to Balance PI3K in B Lineage Cells

(A) A scheme showing the proposed function of the c-Myc/miR17-92/Pten axis (highlighted in red) in controlling PI3K activity and the consequential cell-fate decision for positive and negative selection.

(B) miR-172 and Myc target genes are differentially expressed between CD19 high and low B cells profileGene Set Enrichment Analysis of shared targets of Myc and miR-172 (top) and miR-172 only (bottom) between CD19 high and low B cells profiled by microarray (false discovery rate [FDR] <0.1, p values and normalized enrichment scores of 1.47, $p < 0.02$, and 1.35, $p < 0.07$, respectively). The transcriptome profile is indicated by the red-blue bar at the bottom of each plot, running from CD19 high to low. Vertical black lines, the distribution of the gene set within this profile; green, the enrichment profile.

(C and D) Splenic B cells from WT or CD19KO mice were cultured for 6 hr in the presence or absence of GSK3 inhibitor Bio-acetoxime, lyzed, and analyzed by western blotting for the indicated proteins (C) or by qPCR for expression of Pten mRNA and mature miR19b (D). Pten and c-Myc bands detected by western blots were quantified and normalized to their respective actin bands, and fold change for CD19KO and CD19KO+GSK3inh was calculated relative to control ($CD19^{+/+}$) cells. Shown in (C) are representative results and summary of three experiments (mean ± SEM (*$p < 0.05$ from control).

(E) Splenic B cells from WT mice were cultured for 16 hr in the presence or absence of antisense c-Myc oligonucleotides, lysed. and analyzed by qPCR for expression of Pten mRNA and mature miR19b. Results shown are mean ± SE of three experiments.

rescue B cell development in CD19KO mice by inhibiting expression of Pten. To test this, we generated mice deficient of CD19 (homozygous for CD19-cre [Rickert et al., 1995]) that are also homozygous for a miR17-92 transgenic allele, which was inserted into the Rosa26 locus and is conditionally turned on by cre-mediated recombination in B cells (CD19KO miR17-92Tg/Tg) (Xiao et al., 2008). To assess whether PI3K signaling is restored during B cell development, we generated interleukin-7 (IL-7)-driven BM cultures from control, CD19KO, and CD19KO miR17-92Tg/Tg mice. Phospho-flow analysis revealed that upon BCR stimulation the impaired Akt phosphorylation that was evident in immature immunoglobulin M^+ (IgM^+) CD19KO B cells was restored in CD19KO miR17-92Tg/Tg immature B cells (Figures 3A and 3B). Further, Pten expression, which was high in CD19KO B cells, was repressed and c-Myc expression, which was suppressed in CD19KO B cells, was enhanced in CD19KO miR17-92Tg/Tg B cells (Figure 3C). This suggests that overexpression of miR17-92 restored PI3K activity in developing B cells deficient of CD19 via negative regulation of Pten expression.

Next, to address whether restoration of PI3K activity in CD19-deficient cells by overexpression of miR17-92 can rescue B cell development and positive selection in CD19KO mice, we analyzed peripheral B cell populations in control, CD19KO, and CD19KO miR17-92Tg/Tg mice. The results, summarized in Figure 4, showed that the majority of the impairments in B cell development that were readily observed in CD19KO mice were rescued by overexpression of miR17-92. We found that spleen cell cellularity in CD19KO miR17-92Tg/Tg mice, as measured by spleen cell size and total cell numbers (Figures 4B and 4D) and percentages of total splenic B cells ($B220^+$; Figure 4A) were completely restored to normal levels. Further analysis for specific B cell subsets in the spleen revealed that sizes of the mature B2, follicular (FO), and transitional B cells that are severely reduced in CD19KO mice were restored to normal sizes in CD19KO miR17-92Tg/Tg mice (Figures 4C and 4D). Moreover, in the peritoneal cavity the B1a cell subset, which was nearly completely absent in CD19KO mice (Rickert et al., 1995), was partially restored in CD19KO miR17-92Tg/Tg mice (Figure 4E). Interestingly, in CD19KO mice expressing one copy of the miR17-92 transgene we observed an intermediate phenotype of partial restoration for each of these B cell subsets (Figures 4D and S3), suggesting that miR17-92 dosage is critical to fully supplement PI3K activity in CD19KO mice. However, development of the marginal zone (MZ) B cell subset was not rescued in CD19KO miR17-92Tg/Tg mice as compared to CD19KO (Figures 4C and 4D). Last, B cell responsiveness was also not rescued in CD19KO miR17-92Tg/Tg mice as evidenced by lack of germinal center B cells in the spleen upon sheep red

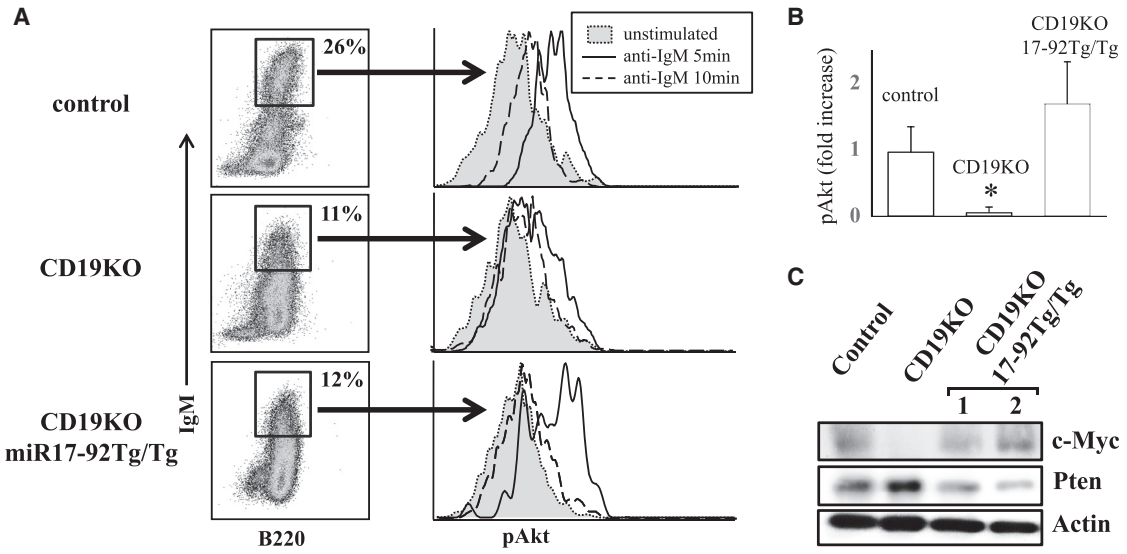

Figure 3. Overexpression of miR17-92 Reconstitutes PI3K Activity in CD19KO Immature B Cells

IL-7-driven BM cultures were prepared from mice of the indicated genotypes.

(A) Cells grown in cultures were stimulated with fluorescently labeled anti-IgM antibodies for 5 and 10 min, fixed, and subsequently stained intracellular for pAkt. Flow cytometry analysis for pAkt gated on immature B cells that were revealed by IgM fluorescence.

(B) Summary of increment in pAkt after 5 min of stimulation calculated as (MFI pAkt stimulation – MFI pAkt unstimulated)/MFI pAkt unstimulated (*$p < 0.05$).

(C) Cells grown in cultures were lysed and analyzed for the indicated proteins by western blotting. Shown are representative results from individual mice (n = 3 in each group).

blood cell (SRBC) priming and complete absence of IgG1 in serum (Figures 4F and 4G), whereas other antibody isotypes were detected (Figure S3). These results indicate that enhancing PI3K activity by overexpression of miR17-92 rescues B cell developmental impairments that are imposed by CD19 deficiency but not B cell activation defects.

The c-Myc/miR17-92/Pten Loop Regulates AICD in B Lineage Cells

Antigen receptor signaling is required not only for developmental progression of B cells but also to eliminate self-reactivity. Ligation of the BCR by autoantigens induces AICD in immature B cells (Edry and Melamed, 2004; Monroe, 2006; Nemazee, 2000), a process that is regulated mainly by the PI3K pathway (Cheng et al., 2009; Clayton et al., 2002; Pogue et al., 2000). In agreement with these results, we showed that immature B cells deficient of CD19, mount increased sensitivity to BCR-induced AICD relative to control cells (about 1.5-fold; Figure 5A). Based on these results, we postulated that the c-Myc/miR17-92/Pten axis, which we showed to balance the PI3K pathway, may also function to tune the threshold to AICD in immature B cells.

To test this mechanistically, we used the immature B lymphoma cell line WEHI-231, previously shown to undergo AICD in response to BCR ligation and used as model for B cell negative selection (Benhamou et al., 1994; Hasbold and Klaus, 1990). Knockdown (kd) of CD19 in these cells effectively suppressed the PI3K pathway as revealed by altered phosphorylation of Akt, GSK3, and reduced expression of c-Myc in response to BCR ligation (Figure S4). We found that suppression of PI3K in $CD19^{kd}$ cells reduces activity of the c-Myc/miR17-92/Pten axis, as indicated by reduced expression of miR19b (Figure 5B) and increased expression of Pten mRNA and protein (Figures 5B and 5C) in $CD19^{kd}$ cells relative to $CD19^{wt}$ cells.

Moreover, the impaired PI3K activity in $CD19^{kd}$ cells resulted in a heightened sensitivity to AICD, as revealed by a 2-fold increase in apoptosis relative to $CD19^{wt}$ cells (Figure 5D). To support the role of the c-Myc/miR17-92/Pten axis in mediating the increased AICD in $CD19^{kd}$ cells, we show that a GSK3 inhibitor effectively rescued both $CD19^{kd}$ and $CD19^{wt}$ WEHI cells from AICD as revealed by a 50% reduction in apoptosis (Figure 5D). Moreover, suppression of Pten expression upon infection with a vector encoding Pten-specific short hairpin RNA (shRNA) (shPten [Fellmann et al., 2013]) rescued from AICD, whereas overexpression of Pten upon infection with a vector encoding human Pten (Pten-OE [Furnari et al., 1997]) enhanced AICD in WEHI cells upon anti-IgM treatment (Figures 5E and 6G). Further experiments using a PI3K inhibitor in control $CD19^{wt}$ cells recapitulated the increased AICD and the impaired Akt/GSK3/c-Myc activation (Figure S4) observed in $CD19^{kd}$ cells. In addition, we found that knockdown of CD19 in AICD-resistant human and mouse cells suppressed PI3K activity and conferred significant sensitivity to AICD (Figure S5). From this, we concluded that knockdown of CD19 suppresses PI3K due to a reduced activity of the c-Myc/miR17-92/Pten axis, which leads to increased expression of Pten and results in increased sensitivity to AICD, a process reversible by altering the activity of the c-Myc/miR17-92/Pten axis.

To further confirm these findings, we performed the reciprocal experiment where we transfected WEHI-231 cells with human CD19 (hCD19) to overexpress functional CD19 in these

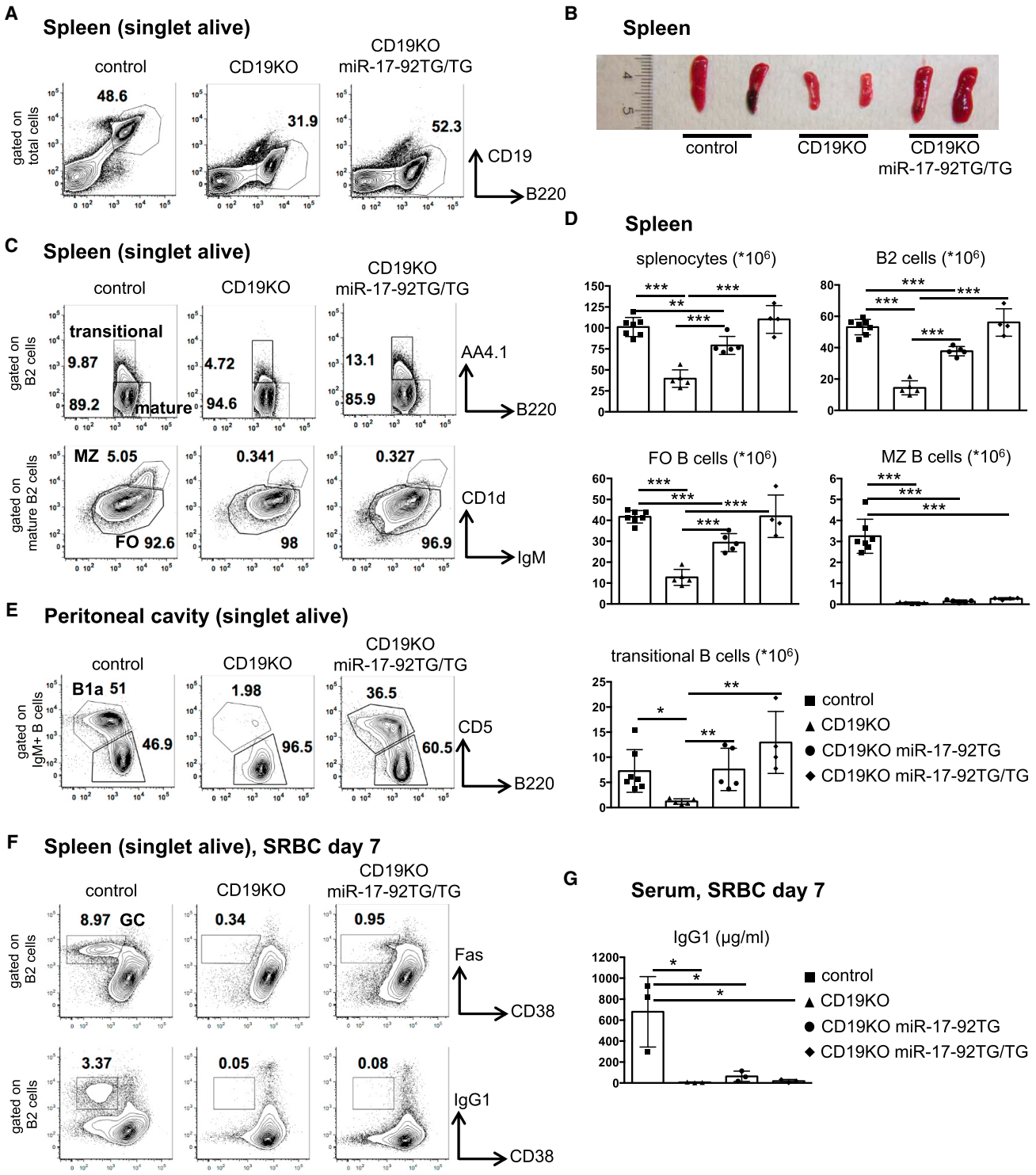

Figure 4. Partial Rescue of CD19KO B Cells by miR17-92 Overexpression

(A) Representative flow cytometry analysis of splenocytes from the indicated genotypes shows presence/absence of cell-surface CD19 expression on $B220^+$ B cells. Numbers adjacent to outlined areas indicate percentage of cells among total splenocytes in each gate.

(B) Spleens of mice of the indicated genotypes; two spleens per genotype are shown.

(C) Representative flow cytometry analysis of splenocytes from the indicated genotypes shows percentage of cells among total splenocytes for transitional B cells ($B220^+AA4.1^+$), mature B2 B cells ($B220^+AA4.1^-$), follicular (FO) B cells ($B220^+AA4.1^-IgM^+CD1d^{low}$), and marginal zone (MZ) B cells ($B220^+AA4.1^-IgM^+CD1d^{high}$).

(legend continued on next page)

cells. Cells overexpressing CD19 that were sorted (Figure 5F) exhibited augmented PI3K activity as revealed by increased phosphorylation of Akt, GSK3, and consequential elevation in expression of c-Myc (Figure S6). Further, we found in hCD19^{+} cells increased expression of miR19b (Figure 5G) and reduced expression of Pten mRNA and protein (Figures 5G and 5H), suggesting that the enhanced PI3K in hCD19^{+} cells may reflect the augmented activity of the c-Myc/miR17-92/Pten axis. Upon ligation of the BCR, we found that overexpression of CD19 and the consequential enhancement of the PI3K pathway conferred partial resistance to AICD. Thus, while 33% apoptosis were recorded in the control (hCD19^{-}) cells, the fraction of apoptotic cells overexpressing CD19 was reduced by 50% (Figure 5F). Taken together, these data suggest that the c-Myc/miR17-92/Pten axis regulates the sensitivity of B cells to AICD and that alteration of this axis, such as by modification of CD19 expression, may affect cell-fate decisions.

Altering Expression of miR17-92 Modifies PI3K Activity and Sensitivity to AICD

To reveal the role of the c-Myc/miR17-92/Pten axis in controlling PI3K-mediated AICD, we modified miR17-92 expression. Ectopic overexpression of miR17-92 in the AICD-sensitive WEHI-231 cells suppressed Pten expression (Figure 6A) and led to augmented PI3K activity (Figure 6B). This was also supported by increased phosphorylation and inactivation of GSK3 and elevation of c-Myc expression, which was sustained at high level even after BCR ligation (Figure 6C). In agreement with an earlier study (Kluiver and Chen, 2012), we show that upon ligation of the BCR the augmented PI3K activity, which was obtained here by overexpression of miR17-92, effectively conferred protection from AICD as apoptosis rates were reduced by about 50% (Figure 6D).

In a reciprocal experiment, we infected WEHI-231 cells with the miR19b-sponge encoding vector (Kluiver et al., 2012) to reduce expression of this miRNA. We found that expression of Pten is increased in these cells (Figure 6E). Further, upon BCR ligation we observed a significant increase in apoptosis (Figure 6F). This increase, however, was blocked in cells co-transfected with miR19b-sponge and shPten (Figures 6F and 6G), suggesting that the increased apoptosis induced by the miR19b-sponge is mediated via the alteration of Pten expression. Taken together, these findings further support the major role of the c-Myc/miR17-92/Pten axis in balancing PI3K activity and setting the threshold for AICD in B lineage cells. Altering this axis, such as by overexpression of miR17-92 or suppression of miR19b, effectively confers Pten-mediated protection or sensitivity, respectively, to AICD.

Overexpression of miR17-92 Protects Immature CD19KO B Cells from AICD

Finally, to confirm the physiological relevance of the c-Myc/miR17-92/Pten axis in controlling AICD, we stimulated immature B cells from control, CD19KO, and CD19KO miR17-92Tg/Tg mice that where grown in BM cultures with anti-BCR antibodies and monitored apoptosis rates. Overexpression of miR17-92, which restores the impaired PI3K activity in CD19KO B cells (Figures 3 and 4), protected immature B cells that are deficient of CD19 from AICD (Figure 7). Thus, the heightened sensitivity to BCR-mediated AICD that is evident in immature CD19KO B cells (Figure 7, compared to control $p < 0.05$) was replaced by an AICD-resistant phenotype, which we observed in cultures of immature CD19KO miR17-92Tg/Tg B cells ($p < 0.02$, compared to CD19KO).

DISCUSSION

Here, we show a regulatory loop by which the PI3K pathway controls itself through post-transcriptional regulation of Pten in normal B cell development. This loop connects a transcription factor (c-Myc), a miRNA cluster (miR17-92) and a signaling molecule (Pten) and functions by tuning PI3K activity to determine life and death decisions in developing B cells during positive and negative selection. Moreover, we show that miR17-92 overexpression amplifies this axis to effectively compensate for the impaired PI3K activity in CD19KO mice and to reconstitute most of the B cell developmental impairments that are evident in these mice. This provides evidence that miRNAs, by altering intracellular biochemical pathways, are capable in restoring severe developmental impairments that result from deficiency of an important regulatory protein.

miR17-92 is essential for B cell development (Ventura et al., 2008). We show here that miR17-92 participates in the Pten-mediated regulation of the PI3K pathway, via the c-Myc/miR17-92/Pten axis, to control positive and negative selection of B lineage cells. This is evidenced by our findings that ablation of Dicer in transitional B cells enhances Pten expression and the observation that Pten expression level is inversely affected by the level of PI3K activity upon suppression or overexpression of CD19. Using multiple approaches, we show that the cross-talk between the PI3K pathway and Pten is mediated via miR17-92. The mechanism of this regulation is proposed in Figure 2A. Accordingly, c-Myc, whose levels are regulated by PI3K activity (Sears, 2004), stimulates miR17-92 expression, which promotes degradation of Pten mRNA to dampen Pten protein levels. Most importantly, our results validate the physiological relevance of this major axis in vivo. In CD19KO miR17-92Tg/Tg mice, PI3K activity is likely increased as a consequence of Pten suppression

(D) Graphs depict total cell numbers of the respective splenic subpopulations shown in (C) as well as total splenocyte numbers (n = 4–7).
(E) Representative flow cytometry analysis from the indicated genotypes shows percentage of cells among peritoneal cavity derived cells for B1a B cells (IgM^{+}B220$^{+/low}$CD5^{+}).
(F) Representative flow cytometry analysis from mice of the indicated genotypes on day 7 upon immunization with sheep red blood cells (SRBCs) shows percentage of cells among total splenocytes for germinal center (GC) B cells (B220^{+}CD38^{low}Fas^{high}) and class switched IgG1^{+} B cells (B220^{+}CD38^{low}IgG1^{+}).
(G) Graph depicts Serum IgG1 levels of the indicated genotypes on day 7 upon immunization with SRBC (n = 3).
All plots are gated on alive singlets. Graphs depict mean values and SDs of the respective populations. Significance was calculated by the two-tailed Student's t test (*$p < 0.05$; **$p < 0.01$; ***$p < 0.001$).

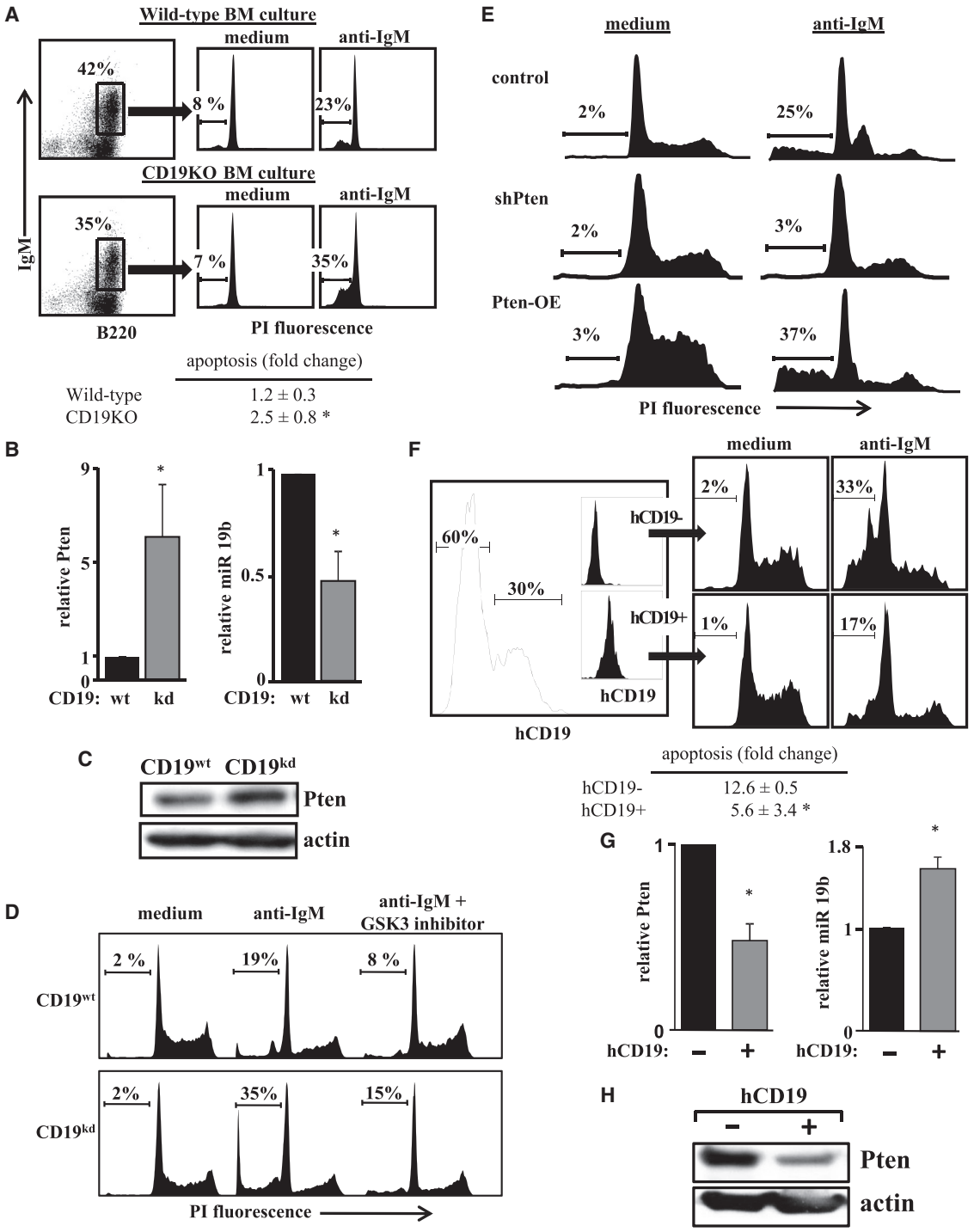

Figure 5. Modification of CD19 Expression Alters c-Myc/miR17-92/Pten Axis Activity and the Consequential Sensitivity to AICD

(A) BM cultures from WT and CD19KO mice were grown for 5 days in the presence of IL-7. Immature B cells ($B220^{+}IgM^{+}$) were sorted and cultured in the presence or absence of anti-IgM antibodies for 16 hr, and apoptosis rates were determined by PI stain. Shown are representative results from individual mice and summary of group results (n = 3 in each group) expressed as mean ± SE (*$p < 0.05$).

(B and C) $CD19^{wt}$ and $CD19^{kd}$ WEHI 231 cells were lysed and analyzed by qPCR for Pten mRNA and mature miR19b (B) and for Pten protein expression by western blotting (C). Results shown are mean ± SE of three experiments.

(D) $CD19^{wt}$ and $CD19^{kd}$ WEHI 231 cells were treated for 16 hr with anti-IgM antibodies in the presence or absence of the GSK3 inhibitor Bio-acetoxime and analyzed for apoptosis by PI stain. Results are representative of three experiments.

(legend continued on next page)

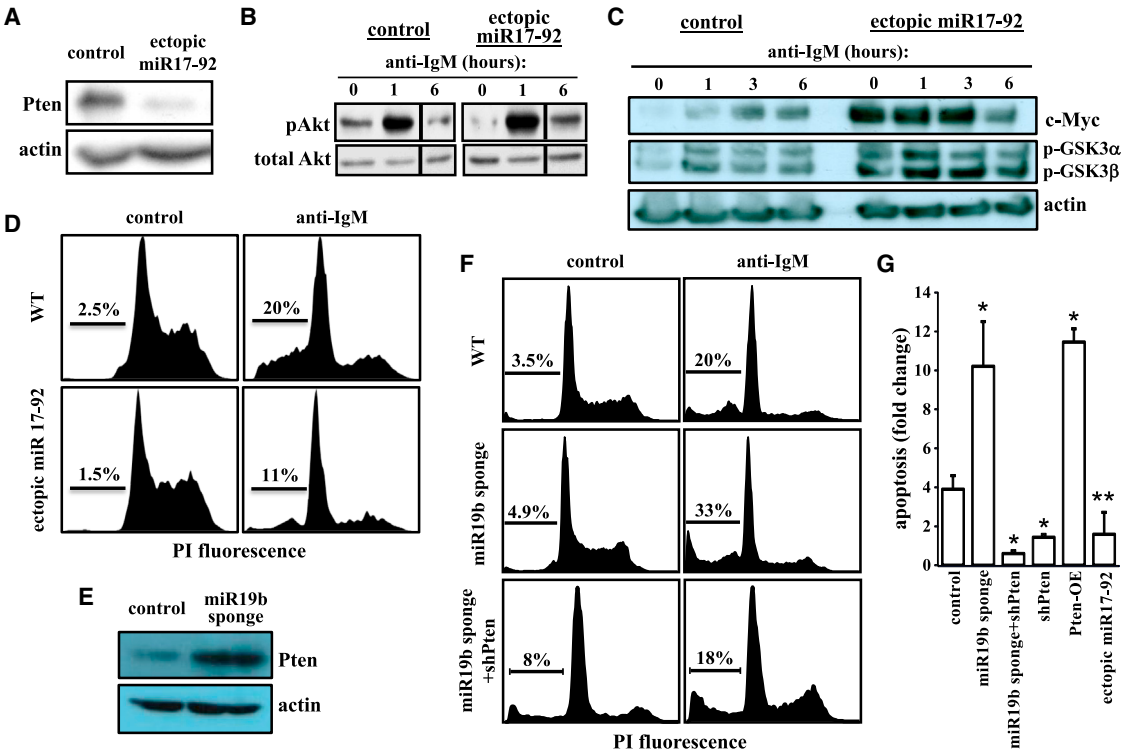

Figure 6. Modification of miR17-92 Expression Alters c-Myc/miR17-92/Pten Axis Activity and the Consequential Sensitivity to AICD

(A–D) WEHI-231 cells were infected with a viral vector to ectopically overexpress miR17-92. Control and ectopic miR17-92 WEHI 231 cells were lysed, and expression of Pten protein was determined by western blotting (A), or the cells were stimulated with anti-IgM antibodies for the indicated time intervals lysed and analyzed for pAkt (B, black line indicates assembly of different lanes from same blot) or the indicated proteins by western blotting (C), or the cells were stimulated with anti-IgM antibodies for 16 hr and analyzed for apoptosis by PI stain (D).

(E and F) WEHI-231 cells were infected with a viral vector encoding a sponge system to miR19b. Control and miR19b sponge WEHI-231 cells were lysed to determine Pten protein expression by western blotting (E), or the cells were stimulated with anti-IgM antibodies for 16 hr and analyzed for apoptosis by PI stain (F).

(G) Summary of PI results of WEHI cells infected with the indicated constructs upon anti-IgM stimulation. Shown are mean results from three to four repeats ±SE. Significance shown is *$p < 0.001$; **$p < 0.05$ as calculated by Wilcoxon rank-sum test.

(Figure 3), and most of the B cell developmental impairments that are evident in CD19KO mice are rescued (Figure 4). The finding that this rescue depends on miR17-92 dosage (Figure 4D) supports the physiological relevance of this regulation and signifies this finding. There are several other studies generally supporting the relevance of this axis in regulating PI3K activity in B cells. (1) Conditional overexpression of miR17-92 suppresses Pten and leads to augmented PI3K signals and tumorigenesis (Jin et al., 2013; Xiao et al., 2008). (2) In vivo ablation of Pten restores B1a and MZ B cell development and activity in $CD19^{-/-}$ mice (Anzelon et al., 2003). (3) Constitutively active PI3K or Pten deletion effectively enhance PI3K activity to rescue BCR-deleted mature B cells in vivo (Srinivasan et al., 2009). While these studies reveal the importance of tonic PI3K signals for normal B cell development and survival, our findings uncover an intracellular mechanism by which these tonic signals might be balanced and the central role of miR17-92 in establishing it.

In striking contrast to the rescue of B1a and B2 cell development, the MZ B cell population was not rescued in CD19KO miR17-92Tg/Tg mice (Figure 4). The MZ B cells comprise a small subset of cells residing in the marginal zone of the spleen whose development depends on BCR signal strength that is driven by binding to self-antigen (Dammers and Kroese, 2005; Martin and Kearney, 2002). Interestingly, and in contrast to our results,

(E) WEHI-231 cells were transfected with a shPten vector to knock down Pten expression, or with an inducible Tet-on vector to overexpress Pten (Pten-OE). Control and shPten cells were cultured for 12 hr with or without anti-IgM antibodies, and apoptosis rates were determined by PI stain. Pten-OE cells were co-treated for 12 hr with doxycycline (to induce Pten expression) and with or without anti-IgM antibodies, and apoptosis rates were determined by PI stain. Summary of repeats and statistics are shown in Figure 6G.

(F–H) WEHI-231 cells were infected with a viral vector to overexpress hCD19 (Supplemental Experimental Procedures). Cells were stained with antibodies to hCD19 and sorted to $hCD19^{-}$ and $hCD19^{+}$ as shown (F). Sorted cells were then treated with anti-IgM antibodies for 16 hr and analyzed for apoptosis by PI stain. Shown are representative results from individual mice and summary of three experiments expressed as mean ± SE (*$p < 0.05$) (F). $hCD19^{+}$ and $hCD19^{-}$ WEHI 231 cells were lysed and analyzed by qPCR for Pten mRNA and mature miR19b (G) and for Pten protein expression by western blotting (H). Results shown are mean ± SE of three experiments.

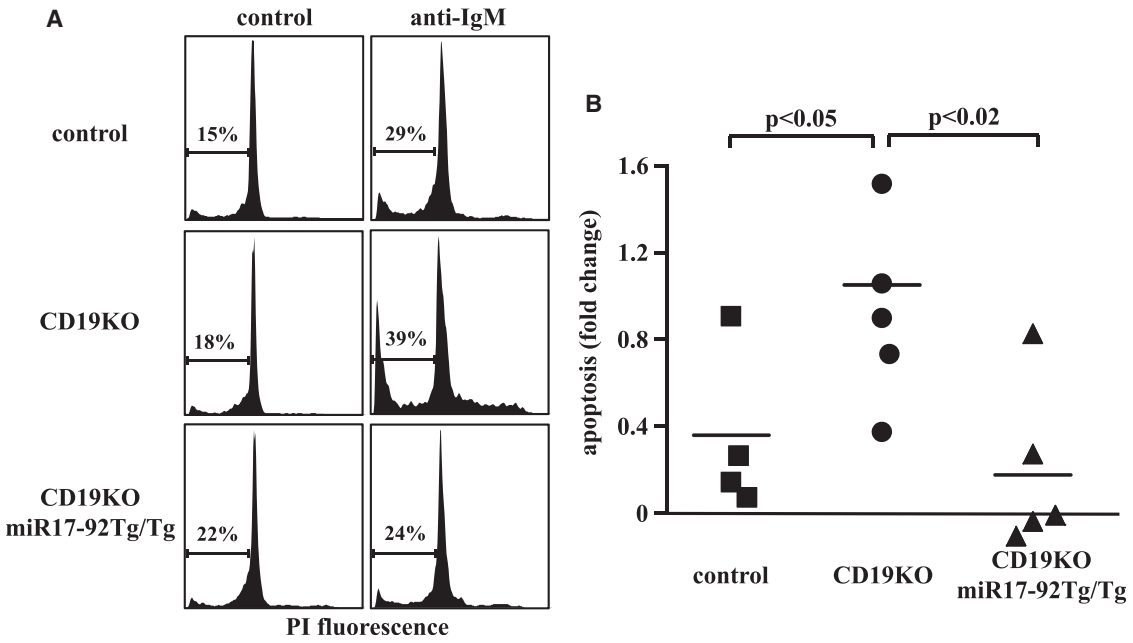

Figure 7. Overexpression of miR17-92 Protects CD19KO B Cells from AICD

(A and B) BM cultures from mice of the indicated genotypes were prepared. Cells grown in cultures were stimulated with fluorescently labeled anti-IgM antibodies for 16 hr, fixed, and stained for apoptosis by PI. Untreated cultures were stained after 16 hr for IgM, fixed, and stained for PI. Flow cytometry analysis for apoptosis was performed and immature B cells were revealed by IgM fluorescence. Shown are representative results for PI analysis (A), and summary of results from individual mice (n = 4–5 in each group) (B). Also shown are p values to indicate statistical differences in apoptosis increase in response to anti-IgM treatment between groups as measured by Wilcoxon rank-sum test.

in CD19KO PtenKO mice MZ B cells development is rescued in addition to B1a and B2 cells (Anzelon et al., 2003). Yet, this apparent contradiction could be explained by the differences in levels of Pten expression. In the CD19KO miR17-92Tg/Tg mice, Pten expression is reduced to a normal, or close to normal, level (Figure 3), whereas in Anzelon et al. Pten is completely ablated in B cells (Anzelon et al., 2003). Since Pten expression level regulates PI3K activity (Suzuki et al., 2008), it is plausible that, in the complete absence of Pten, PI3K activity is strong enough to promote MZ cell differentiation. This notion is supported by the finding that antigen-driven responsiveness of B2 cells was also not reconstituted in CD19KO miR17-92Tg/Tg mice, as was found in in CD19KO PtenKO mice (Anzelon et al., 2003).

Similar to MZ B cells, development of B1a cells is also regulated by strength of BCR signaling, as low signal strength results in a reduced B1a cell subset, whereas enhanced signaling expands this population (Berland and Wortis, 2002; Martin and Kearney, 2001). The finding that B1a cell development is rescued in CD19KO miR17-92Tg/Tg mice (Figure 4) suggests that overexpression of miR17-92 reconstitutes PI3K activity in CD19KO mice, via the c-Myc/miR17-92/Pten axis, to a level that is sufficient to promote development of B1a cells. This is supported by an earlier study showing that conditional deletion of Pten is capable to reconstitute B1a cell development in mice deficient of P110δ catalytic subunit of PI3K (Janas et al., 2008).

In immature B cells undergoing central tolerance, strong BCR signals activate AICD. Our data suggest that CD19 regulates the signaling threshold for AICD in these cells by tuning PI3K activity via the c-Myc/miR17-92/Pten axis. Thus, in the absence of CD19 PI3K is suppressed and immature B cells mount a heightened sensitivity to AICD, whereas overexpression of CD19 enhances PI3K activity and confers protection from AICD (Figure 5), suggesting that CD19 may function as a molecular determinant for cell-fate decision during negative selection. These observations are in agreement with previous studies showing that chemical inhibitors to PI3K enhance AICD in B lineage cells (Carey et al., 2000), and that alterations in CD19 expression are associated with autoimmunity in mouse and human (Inaoki et al., 1997; Saito et al., 2002; Sato et al., 2000). CD19 expression and PI3K activity have also been shown to be important for receptor editing (Verkoczy et al., 2007) and anergy (Browne et al., 2009). Hence, while in CD19KO mice peripheral B cell numbers are reduced as a result of impaired maturation and differentiation (Diamant et al., 2005; Engel et al., 1995; Otero and Rickert, 2003; Rickert et al., 1995; Shivtiel et al., 2002), our findings suggest that enhanced negative selection of immature/transitional B cells by AICD may also contribute to this.

Furthermore, we demonstrate that, via this axis, PI3K controls expression of Pten post-transcriptionally, and that Pten expression level pre-determines sensitivity to AICD. Thus, CD19KO immature B cells mount heightened sensitivity to AICD, whereas in CD19KO miR17-92Tg/Tg Pten expression is reduced to normal level and immature B cells are protected from AICD (Figure 7). Clinically, it has been shown that expression level of CD19 and enhanced PI3K activity contribute to the breakdown of B cell tolerance and production of autoantibodies (Ball et al.,

2014; Sato et al., 2000), and PI3K inhibitors are now used as potential therapeutic drugs for autoimmune diseases (Ball et al., 2014). Our results suggest that some of the therapeutic activities of these PI3K inhibitors might be mediated by the c-Myc/miR17-92/Pten axis.

In this study, we used anti-IgM antibodies to mimic surrogate self-antigen binding for negative selection by AICD, in both primary immature B cells and the WEHI-231 B cell line. It is important to note that the capacity of anti-IgM to kill normal immature B cells in vitro may not accurately reflect negative selection of self-reactive B cells in vivo. Yet, this model for negative selection of normal B cells has been shown to recapitulate self-tolerance mechanisms that were studied in immunoglobulin-transgenic mouse models with known self-specificity (Edry and Melamed, 2004; Monroe, 2006; Nemazee, 2000). Hence, BCR-mediated PI3K activation by self-antigen or by anti-IgM may also function in maintaining self-tolerance as we show here, in addition to its other important roles at various stages of B cell development.

Clearly, Pten activity and Pten protein turnover are regulated by additional mechanisms (Carracedo and Pandolfi, 2008; Papakonstanti et al., 2007; Xu et al., 2010), as well as at the transcriptional level (reviewed in Carracedo and Pandolfi, 2008). Although some or all of these mechanisms may apply to the regulation of Pten in B lineage cells, we believe that c-Myc/miR17-92/Pten is an axis shown to control its expression at the post-transcriptional stage. It is worth noting that other microRNAs, such as miR106 and miR181, were shown to regulate Pten and PI3K activity in other cell lineages, but the mechanism regulating their expression is unclear (Henao-Mejia et al., 2013).

Finally, in addition to positive and negative selection, CD19 expression and PI3K activity are important for B cell lymphoma development and prognosis by enhancing expression of c-Myc (Chung et al., 2012; Poe et al., 2012). Our results suggest that in B cell lymphoma the c-Myc/miR17-92/Pten axis may function as a vicious circle to suppress Pten expression and to maintain enhanced PI3K activity. Indeed, evidence for the tumorigenic function of this axis has been suggested by genomic screening of Burkitt's lymphoma cells (Schmitz et al., 2012). The fact that Pten mutations and deletions are detected in many B cell neoplasms also supports this. Since PI3K inhibitors are now used for treatment of B cell malignancies, it would be interesting to study their effect on this axis. Our results suggest that inhibitors for this axis may also be beneficial to treat cancer B cells.

EXPERIMENTAL PROCEDURES

Mice

CD19KO (homozygous for CD19-cre [Rickert et al., 1995]) and miR17-92Tg mice (Xiao et al., 2008) have been described. All mice are C57BL/6 or have been backcrossed to the C57BL/6 background for more than ten generations. For the depletion-autoreconstitution model, we used mice transgenic for human CD20 (hCD20Tg) (Ahuja et al., 2007). For in vivo Ablation of Dicer and Pten, we used Dicer$^{fl/fl}$ (Murchison et al., 2005) and Pten$^{fl/fl}$ (Trotman et al., 2003) mice that were crossed with Mx-cre transgenic mice (Kühn et al., 1995), enabling ablating the floxed alleles upon in vivo administration of poly(I)-poly(C). For T-dependent immunization experiments, mice were injected once intravenously with 1×10^9 sheep red blood cells (SRBCs; Cedarlane). Mice were housed and bred at the animal facility of the Technion, Faculty of Medicine (Israel) and the Max Delbrück Center for Molecular Medicine (Berlin, Germany) and used for experiments at 7–12 weeks of age. Mouse studies at the Technion were approved by the local committee for the supervision of animal experiments. Animal care in Berlin followed guidelines of the Max Delbrück Center for Molecular Medicine and the governmental review board (Landesamt für Gesundheit und Soziales Berlin, LaGeSo).

Cells and Stimulations

Splenic B cells were purified using a B cell isolation kit (STEMCELL Technologies), cultured in standard DMEM (supplemented with sodium pyruvate, Pen-Strep antibiotics, and 2-mercapthoethanol), and treated as detailed. Cells were lysed for western blotting analysis and for quantification of mRNAs and microRNAs. WEHI-231 cells were cultured in standard DMEM. Cells were infected with different viral vectors to knock down CD19, overexpress hCD19, overexpress miR17-92 or to express a sponge system to miR-19b, overexpress Pten, or knock down Pten. Stable transfectants were selected and used for the experiments. Cells were lysed (see Methodology in the Supplemental Information) for western blotting and quantification of mRNAs and miRNAs. BM cultures for B cell precursors were prepared as previously described (Leider and Melamed, 2003). Cells grown in these primary cultures (>95% B220$^+$) were used as detailed.

Flow Cytometry

Single-cell suspensions from mouse organs were stained with fluorescently labeled antibodies for surface and intracellular proteins to identify specific B cell subsets, quantify level of expression and apoptosis and activation of signaling pathways. Data were acquired on LSRFortessa (BD Pharmingen) and analyzed using FlowJo software (Tree Star). For more details on cell preparations antibodies and flourochromes, see Supplemental Experimental Procedures.

ELISA

Immunoglobulin serum concentrations of SRBC immunized mice were determined as published (Roes and Rajewsky, 1993) (see details in Supplemental Experimental Procedures).

Activation-Induced Cell Death

5×10^5 WEHI-231 transfectants or 5×10^6 BM culture cells were cultured with goat-anti-mouse IgM (10 mg/ml) (Southern Biotechnology Associates) or with the F(ab')2 of goat anti-mouse IgM or with Allophycocyanin (APC)-labeled goat anti-mouse IgM (Jackson ImmunoResearch) for 12 hr to induce AICD. Cells were collected, washed with PBS, and incubated for 10 min in dark with propidium iodine (PI) solution (PBS containing 0.3% saponin, 5 μg/ml propidium iodine, 50 μg/ml RNase, 5 mM EDTA [pH 8]). Apoptotic cells were determined by their hypochromic sub-diploid staining profiles using LSRFortessa, and the collected data were analyzed using FlowJo software. Apoptotic rates for individual mice are expressed by fold increase calculated as (anti-IgM-induced apoptosis – apoptosis in unstimulated)/apoptosis in unstimulated samples.

Statistical Analysis

The statistical significance of the differences between experimental groups was determined using unpaired two-tailed Student's t test with differences considered significant at $p < 0.05$. In some experiments, statistical differences in apoptosis increase between groups was measured using the Wilcoxon rank-sum test using R software.

SUPPLEMENTAL INFORMATION

Supplemental Information includes Supplemental Experimental Procedures, seven figures, and one table and can be found with this article online at http://dx.doi.org/10.1016/j.celrep.2016.05.084.

AUTHOR CONTRIBUTIONS

D.B. and D.M. conceived of the study; D.B. and V.L. designed and carried out most of the experiments and data analysis. R.N., I.D., S.S.-A., and R.A. carried out additional experiments and performed data analysis; A.W. and R.G.

performed gene expression analysis; D.B., V.L., K.R., S.S.S.-O., and D.M. wrote and edited the manuscript.

ACKNOWLEDGMENTS

We would like to acknowledge Veronicca Andrews and Johannes Zuber for providing the shPten vector, Joost Kluiver for providing the miR19b-sponge vector, and Andrea Ventura for providing the miR17-92 vector. We are grateful to Eli Benchetrit, Claudia Grosse, and Janine Cernoch for technical support, and to Emmanuel Derudder for helpful discussions. This work was supported by grants from the Israel Science Foundation (1408/13), the Cooperation Program in Cancer Research of the Israeli Ministry of Science Culture and Sports (MOST) and the Deutsches Krebsforschungszentrum (DKFZ) Heidelberg Germany, and the Colleck Research Fund to D.M., and by an ERC Advanced Grant 268921 to K.R.

Received: February 29, 2016
Revised: April 14, 2016
Accepted: May 19, 2016
Published: June 23, 2016

REFERENCES

Ahuja, A., Shupe, J., Dunn, R., Kashgarian, M., Kehry, M.R., and Shlomchik, M.J. (2007). Depletion of B cells in murine lupus: efficacy and resistance. J. Immunol. *179*, 3351–3361.

Alkhatib, A., Werner, M., Hug, E., Herzog, S., Eschbach, C., Faraidun, H., Köhler, F., Wossning, T., and Jumaa, H. (2012). FoxO1 induces Ikaros splicing to promote immunoglobulin gene recombination. J. Exp. Med. *209*, 395–406.

Anzelon, A.N., Wu, H., and Rickert, R.C. (2003). Pten inactivation alters peripheral B lymphocyte fate and reconstitutes CD19 function. Nat. Immunol. *4*, 287–294.

Ball, J., Archer, S., and Ward, S. (2014). PI3K inhibitors as potential therapeutics for autoimmune disease. Drug Discov. Today *19*, 1195–1199.

Benhamou, L.E., Watanabe, T., Kitamura, D., Cazenave, P.A., and Sarthou, P. (1994). Signaling properties of anti-immunoglobulin–resistant variants of WEHI-231 B lymphoma cells. Eur. J. Immunol. *24*, 1993–1999.

Berland, R., and Wortis, H.H. (2002). Origins and functions of B-1 cells with notes on the role of CD5. Annu. Rev. Immunol. *20*, 253–300.

Browne, C.D., Del Nagro, C.J., Cato, M.H., Dengler, H.S., and Rickert, R.C. (2009). Suppression of phosphatidylinositol 3,4,5-trisphosphate production is a key determinant of B cell anergy. Immunity *31*, 749–760.

Buhl, A.M., Pleiman, C.M., Rickert, R.C., and Cambier, J.C. (1997). Qualitative regulation of B cell antigen receptor signaling by CD19: selective requirement for PI3-kinase activation, inositol-1,4,5-trisphosphate production and Ca2+ mobilization. J. Exp. Med. *186*, 1897–1910.

Carey, G.B., Donjerković, D., Mueller, C.M., Liu, S., Hinshaw, J.A., Tonnetti, L., Davidson, W., and Scott, D.W. (2000). B-cell receptor and Fas-mediated signals for life and death. Immunol. Rev. *176*, 105–115.

Carracedo, A., and Pandolfi, P.P. (2008). The PTEN-PI3K pathway: of feedbacks and cross-talks. Oncogene *27*, 5527–5541.

Cheng, S., Hsia, C.Y., Feng, B., Liou, M.L., Fang, X., Pandolfi, P.P., and Liou, H.C. (2009). BCR-mediated apoptosis associated with negative selection of immature B cells is selectively dependent on Pten. Cell Res. *19*, 196–207.

Chung, E.Y., Psathas, J.N., Yu, D., Li, Y., Weiss, M.J., and Thomas-Tikhonenko, A. (2012). CD19 is a major B cell receptor-independent activator of MYC-driven B-lymphomagenesis. J. Clin. Invest. *122*, 2257–2266.

Clayton, E., Bardi, G., Bell, S.E., Chantry, D., Downes, C.P., Gray, A., Humphries, L.A., Rawlings, D., Reynolds, H., Vigorito, E., and Turner, M. (2002). A crucial role for the p110δ subunit of phosphatidylinositol 3-kinase in B cell development and activation. J. Exp. Med. *196*, 753–763.

Cyster, J.G., Healy, J.I., Kishihara, K., Mak, T.W., Thomas, M.L., and Goodnow, C.C. (1996). Regulation of B-lymphocyte negative and positive selection by tyrosine phosphatase CD45. Nature *381*, 325–328.

Dammers, P.M., and Kroese, F.G.M. (2005). Recruitment and selection of marginal zone B cells is independent of exogenous antigens. Eur. J. Immunol. *35*, 2089–2099.

Diamant, E., Keren, Z., and Melamed, D. (2005). CD19 regulates positive selection and maturation in B lymphopoiesis: lack of CD19 imposes developmental arrest of immature B cells and consequential stimulation of receptor editing. Blood *105*, 3247–3254.

Donjerković, D., and Scott, D.W. (2000). Activation-induced cell death in B lymphocytes. Cell Res. *10*, 179–192.

Edry, E., and Melamed, D. (2004). Receptor editing in positive and negative selection of B lymphopoiesis. J. Immunol. *173*, 4265–4271.

Eeva, J., and Pelkonen, J. (2004). Mechanisms of B cell receptor induced apoptosis. Apoptosis *9*, 525–531.

Engel, P., Zhou, L.J., Ord, D.C., Sato, S., Koller, B., and Tedder, T.F. (1995). Abnormal B lymphocyte development, activation, and differentiation in mice that lack or overexpress the CD19 signal transduction molecule. Immunity *3*, 39–50.

Fellmann, C., Hoffmann, T., Sridhar, V., Hopfgartner, B., Muhar, M., Roth, M., Lai, D.Y., Barbosa, I.A., Kwon, J.S., Guan, Y., et al. (2013). An optimized microRNA backbone for effective single-copy RNAi. Cell Rep. *5*, 1704–1713.

Furnari, F.B., Lin, H., Huang, H.S., and Cavenee, W.K. (1997). Growth suppression of glioma cells by PTEN requires a functional phosphatase catalytic domain. Proc. Natl. Acad. Sci. USA *94*, 12479–12484.

Hasbold, J., and Klaus, G.G. (1990). Anti-immunoglobulin antibodies induce apoptosis in immature B cell lymphomas. Eur. J. Immunol. *20*, 1685–1690.

Henao-Mejia, J., Williams, A., Goff, L.A., Staron, M., Licona-Limón, P., Kaech, S.M., Nakayama, M., Rinn, J.L., and Flavell, R.A. (2013). The microRNA miR-181 is a critical cellular metabolic rheostat essential for NKT cell ontogenesis and lymphocyte development and homeostasis. Immunity *38*, 984–997.

Herzog, S., Hug, E., Meixlsperger, S., Paik, J.-H., DePinho, R.A., Reth, M., and Jumaa, H. (2008). SLP-65 regulates immunoglobulin light chain gene recombination through the PI(3)K-PKB-Foxo pathway. Nat. Immunol. *9*, 623–631.

Inaoki, M., Sato, S., Weintraub, B.C., Goodnow, C.C., and Tedder, T.F. (1997). CD19-regulated signaling thresholds control peripheral tolerance and autoantibody production in B lymphocytes. J. Exp. Med. *186*, 1923–1931.

Janas, M.L., Hodson, D., Stamataki, Z., Hill, S., Welch, K., Gambardella, L., Trotman, L.C., Pandolfi, P.P., Vigorito, E., and Turner, M. (2008). The effect of deleting p110δ on the phenotype and function of PTEN-deficient B cells. J. Immunol. *180*, 739–746.

Jin, H.Y., Oda, H., Lai, M., Skalsky, R.L., Bethel, K., Shepherd, J., Kang, S.G., Liu, W.-H., Sabouri-Ghomi, M., Cullen, B.R., et al. (2013). MicroRNA-17∼92 plays a causative role in lymphomagenesis by coordinating multiple oncogenic pathways. EMBO J. *32*, 2377–2391.

Kluiver, J.L., and Chen, C.Z. (2012). MicroRNAs regulate B-cell receptor signaling-induced apoptosis. Genes Immun. *13*, 239–244.

Kluiver, J., Gibcus, J.H., Hettinga, C., Adema, A., Richter, M.K.S., Halsema, N., Slezak-Prochazka, I., Ding, Y., Kroesen, B.-J., and van den Berg, A. (2012). Rapid generation of microRNA sponges for microRNA inhibition. PLoS ONE *7*, e29275.

Koralov, S.B., Muljo, S.A., Galler, G.R., Krek, A., Chakraborty, T., Kanellopoulou, C., Jensen, K., Cobb, B.S., Merkenschlager, M., Rajewsky, N., and Rajewsky, K. (2008). Dicer ablation affects antibody diversity and cell survival in the B lymphocyte lineage. Cell *132*, 860–874.

Kühn, R., Schwenk, F., Aguet, M., and Rajewsky, K. (1995). Inducible gene targeting in mice. Science *269*, 1427–1429.

Leider, N., and Melamed, D. (2003). Differential c-Myc responsiveness to B cell receptor ligation in B cell-negative selection. J. Immunol. *171*, 2446–2452.

Martin, F., and Kearney, J.F. (2001). B1 cells: similarities and differences with other B cell subsets. Curr. Opin. Immunol. *13*, 195–201.

Martin, F., and Kearney, J.F. (2002). Marginal-zone B cells. Nat. Rev. Immunol. *2*, 323–335.

Monroe, J.G. (2006). ITAM-mediated tonic signalling through pre-BCR and BCR complexes. Nat. Rev. Immunol. *6*, 283–294.

Murchison, E.P., Partridge, J.F., Tam, O.H., Cheloufi, S., and Hannon, G.J. (2005). Characterization of Dicer-deficient murine embryonic stem cells. Proc. Natl. Acad. Sci. USA *102*, 12135–12140.

Nemazee, D. (2000). Receptor selection in B and T lymphocytes. Annu. Rev. Immunol. *18*, 19–51.

O'Donnell, K.A., Wentzel, E.A., Zeller, K.I., Dang, C.V., and Mendell, J.T. (2005). c-Myc-regulated microRNAs modulate E2F1 expression. Nature *435*, 839–843.

Okkenhaug, K., and Vanhaesebroeck, B. (2003). PI3K in lymphocyte development, differentiation and activation. Nat. Rev. Immunol. *3*, 317–330.

Otero, D.C., and Rickert, R.C. (2003). CD19 function in early and late B cell development. II. CD19 facilitates the pro-B/pre-B transition. J. Immunol. *171*, 5921–5930.

Otero, D.C., Omori, S.A., and Rickert, R.C. (2001). Cd19-dependent activation of Akt kinase in B-lymphocytes. J. Biol. Chem. *276*, 1474–1478.

Papakonstanti, E.A., Ridley, A.J., and Vanhaesebroeck, B. (2007). The p110delta isoform of PI 3-kinase negatively controls RhoA and PTEN. EMBO J. *26*, 3050–3061.

Poe, J.C., Minard-Colin, V., Kountikov, E.I., Haas, K.M., and Tedder, T.F. (2012). A c-Myc and surface CD19 signaling amplification loop promotes B cell lymphoma development and progression in mice. J. Immunol. *189*, 2318–2325.

Pogue, S.L., Kurosaki, T., Bolen, J., and Herbst, R. (2000). B cell antigen receptor-induced activation of Akt promotes B cell survival and is dependent on Syk kinase. J. Immunol. *165*, 1300–1306.

Rickert, R.C., Rajewsky, K., and Roes, J. (1995). Impairment of T-cell-dependent B-cell responses and B-1 cell development in CD19-deficient mice. Nature *376*, 352–355.

Roes, J., and Rajewsky, K. (1993). Immunoglobulin D (IgD)-deficient mice reveal an auxiliary receptor function for IgD in antigen-mediated recruitment of B cells. J. Exp. Med. *177*, 45–55.

Rowland, S.L., Tuttle, K., Torres, R.M., and Pelanda, R. (2013). Antigen and cytokine receptor signals guide the development of the naïve mature B cell repertoire. Immunol. Res. *55*, 231–240.

Saito, E., Fujimoto, M., Hasegawa, M., Komura, K., Hamaguchi, Y., Kaburagi, Y., Nagaoka, T., Takehara, K., Tedder, T.F., and Sato, S. (2002). CD19-dependent B lymphocyte signaling thresholds influence skin fibrosis and autoimmunity in the tight-skin mouse. J. Clin. Invest. *109*, 1453–1462.

Sato, S., Hasegawa, M., Fujimoto, M., Tedder, T.F., and Takehara, K. (2000). Quantitative genetic variation in CD19 expression correlates with autoimmunity. J. Immunol. *165*, 6635–6643.

Schmitz, R., Young, R.M., Ceribelli, M., Jhavar, S., Xiao, W., Zhang, M., Wright, G., Shaffer, A.L., Hodson, D.J., Buras, E., et al. (2012). Burkitt lymphoma pathogenesis and therapeutic targets from structural and functional genomics. Nature *490*, 116–120.

Sears, R.C. (2004). The life cycle of C-myc: from synthesis to degradation. Cell Cycle *3*, 1133–1137.

Shivtiel, S., Leider, N., Sadeh, O., Kraiem, Z., and Melamed, D. (2002). Impaired light chain allelic exclusion and lack of positive selection in immature B cells expressing incompetent receptor deficient of CD19. J. Immunol. *168*, 5596–5604.

Srinivasan, L., Sasaki, Y., Calado, D.P., Zhang, B., Paik, J.H., DePinho, R.A., Kutok, J.L., Kearney, J.F., Otipoby, K.L., and Rajewsky, K. (2009). PI3 kinase signals BCR-dependent mature B cell survival. Cell *139*, 573–586.

Suzuki, A., de la Pompa, J.L., Stambolic, V., Elia, A.J., Sasaki, T., del Barco Barrantes, I., Ho, A., Wakeham, A., Itie, A., Khoo, W., et al. (1998). High cancer susceptibility and embryonic lethality associated with mutation of the PTEN tumor suppressor gene in mice. Curr. Biol. *8*, 1169–1178.

Suzuki, A., Kaisho, T., Ohishi, M., Tsukio-Yamaguchi, M., Tsubata, T., Koni, P.A., Sasaki, T., Mak, T.W., and Nakano, T. (2003). Critical roles of Pten in B cell homeostasis and immunoglobulin class switch recombination. J. Exp. Med. *197*, 657–667.

Suzuki, A., Nakano, T., Mak, T.W., and Sasaki, T. (2008). Portrait of PTEN: messages from mutant mice. Cancer Sci. *99*, 209–213.

Trotman, L.C., Niki, M., Dotan, Z.A., Koutcher, J.A., Di Cristofano, A., Xiao, A., Khoo, A.S., Roy-Burman, P., Greenberg, N.M., Van Dyke, T., et al. (2003). Pten dose dictates cancer progression in the prostate. PLoS Biol. *1*, E59.

Tuveson, D.A., Carter, R.H., Soltoff, S.P., and Fearon, D.T. (1993). CD19 of B cells as a surrogate kinase insert region to bind phosphatidylinositol 3-kinase. Science *260*, 986–989.

Tze, L.E., Schram, B.R., Lam, K.P., Hogquist, K.A., Hippen, K.L., Liu, J., Shinton, S.A., Otipoby, K.L., Rodine, P.R., Vegoe, A.L., et al. (2005). Basal immunoglobulin signaling actively maintains developmental stage in immature B cells. PLoS Biol. *3*, e82.

Ventura, A., Young, A.G., Winslow, M.M., Lintault, L., Meissner, A., Erkeland, S.J., Newman, J., Bronson, R.T., Crowley, D., Stone, J.R., et al. (2008). Targeted deletion reveals essential and overlapping functions of the miR-17 through 92 family of miRNA clusters. Cell *132*, 875–886.

Verkoczy, L., Duong, B., Skog, P., Aït-Azzouzene, D., Puri, K., Vela, J.L., and Nemazee, D. (2007). Basal B cell receptor-directed phosphatidylinositol 3-kinase signaling turns off RAGs and promotes B cell-positive selection. J. Immunol. *178*, 6332–6341.

von Boehmer, H., and Melchers, F. (2010). Checkpoints in lymphocyte development and autoimmune disease. Nat. Immunol. *11*, 14–20.

Werner, M., Hobeika, E., and Jumaa, H. (2010). Role of PI3K in the generation and survival of B cells. Immunol. Rev. *237*, 55–71.

Xiao, C., Srinivasan, L., Calado, D.P., Patterson, H.C., Zhang, B., Wang, J., Henderson, J.M., Kutok, J.L., and Rajewsky, K. (2008). Lymphoproliferative disease and autoimmunity in mice with increased miR-17-92 expression in lymphocytes. Nat. Immunol. *9*, 405–414.

Xu, D., Yao, Y., Jiang, X., Lu, L., and Dai, W. (2010). Regulation of PTEN stability and activity by Plk3. J. Biol. Chem. *285*, 39935–39942.

Cell Reports, Volume *16*

Supplemental Information

A c-Myc/miR17-92/Pten Axis Controls PI3K-Mediated Positive and Negative Selection in B Cell Development and Reconstitutes CD19 Deficiency

David Benhamou, Verena Labi, Rostislav Novak, Isabelle Dai, Shani Shafir-Alon, Ariel Weiss, Renaud Gaujoux, Rüdiger Arnold, Shai S. Shen-Orr, Klaus Rajewsky, and Doron Melamed

Supplementary data and figures

Depletion auto-reconstitution model for transitional B cell generation in vivo.

Mice that are transgenic for human CD20 (hCD20Tg) were injected with mouse anti-human CD20 monoclonal antibodies at 1mg/mouse to deplete all peripheral mature B cells as detailed (1). Depletion of B cells for each mouse was confirmed 3 days later by blood stain to ensure that %B220+ cells is <5%. In these experiments, depleted mice were sacrificed 21 days after antibody injections, a time point when about 50% of the peripheral B cell compartment has been reconstituted from de-novo B lymphopoiesis in the bone marrow (supplementary figure 1, 53% B220+ in control relative to 25% in depleted). As revealed from the results depicted in supplementary figure 1, most of the splenic B cells at this time after depletion are at a transitional stage. This can be concluded from the following: 1) expression level of B220 is reduced by 40 % (B220 MFI for control 6375 and B220 MFI for depleted-autoreconstituted is 3753), 2) In the depleted-autoreconsituted mice 53% of the splenic B cells are transitional IgM^{hi}/IgD^{lo} and only 28% are mature IgM^{lo}/IgD^{hi}, whereas in the control only 23% of the splenic B cells are transitional IgM^{hi}/IgD^{lo} and 73% are mature IgM^{lo}/IgD^{hi}, 3) In the depleted-autoreconsituted mice 46% of the splenic B cells express AA4.1 relative to only 5% in the control, and 4) When treated overnight with anti-IgM antibodies, splenic B cells from the depleted-autoreconstituted mice show heighten sensitivity to AICD as revealed by 39% apoptosis relative to splenic B cells purified from control mice. Hence, similar to the irradiation autoreconstitution mouse model for enrichment of transitional B cells in the spleen that was described (2), our depletion-autoreconstitution model proposes a convenient methodology, that is irradiation-free, to enrich for transitional B cells in the spleen.

Supplementary Figure 1

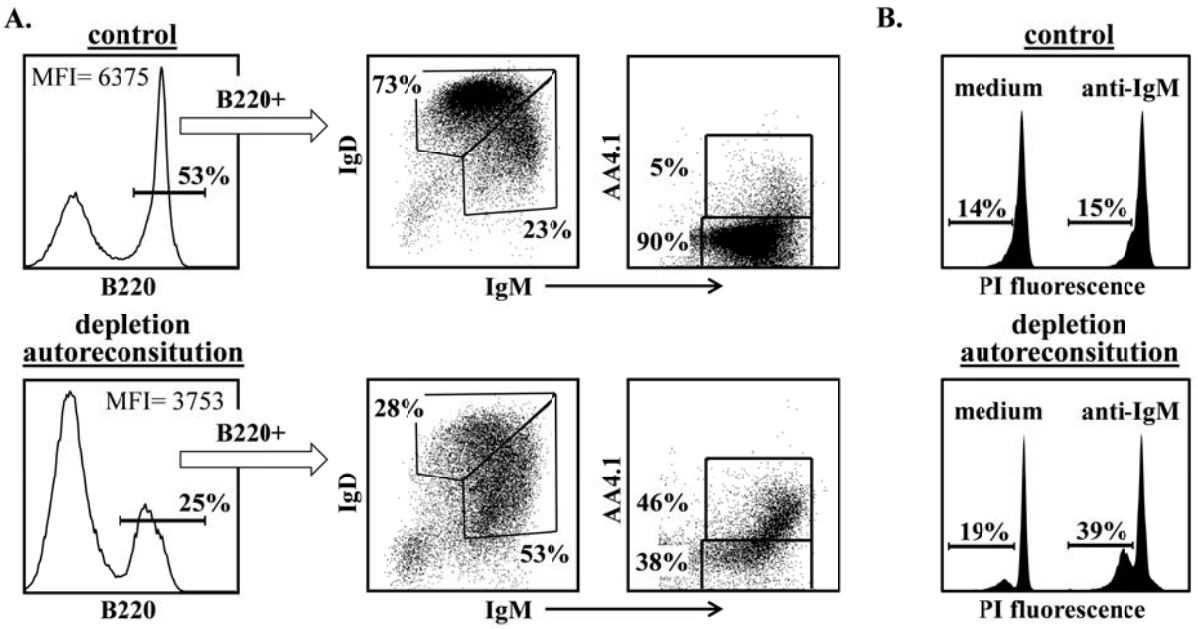

Supplementary figure 1 legend (related to figure 1) – hCD20Tg and wild type control mice were injected with monoclonal mouse anti-human CD20 antibodies (1mg/mouse, intraperitoneal). Depletion of B cells in hCD20Tg mice was confirmed by blood stain 72h after antibody administration (not shown). (A) On day 21, mice were sacrificed and spleen cells were stained for analysis by flow cytometry. (B) Splenic B cells were purified on day 21 after depletion by CD43+ magnetic beads. Purified cells were cultured overnight unstimulated (medium), or in the presence of goat-anti-mouse IgM (10mg/ml), stained by PI and analyzed by flow cytometry.

Absence of microRNAs in B lymphocytes upon inducible ablation of Dicer in mice.

Mice that are Dicer$^{fl/fl}$/Mx-cre were injected on days 7, 10 and 13 mice with poly (I)(C) (400μg/mouse/injection) and splenic B cells were isolated on day 21 and analyzed for expression of miR150, miR29a, and miR19b by qPCR as an indication for Dicer activity. The results in supplementary figure 2 show that upon deletion of Dicer levels of these microRNAs were reduced by 10-70 folds relative to B cells from the control hCD20 mice.

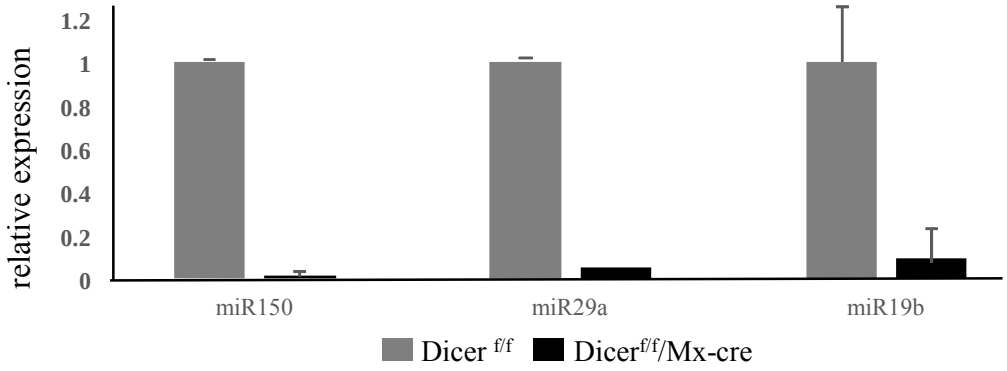

Supplementary figure 2 legend (related to figure 1) – splenic B cells from the indicated mice were lysed and analyzed by qPCR for expression of the indicated microRNAs. Relative expression was calculated using U6 small nuclear RNA as the endogenous reference gene.

Conditional overexpression of miR17-92 rescues B cell development in CD19KO mice.

Supplementary Figure 3

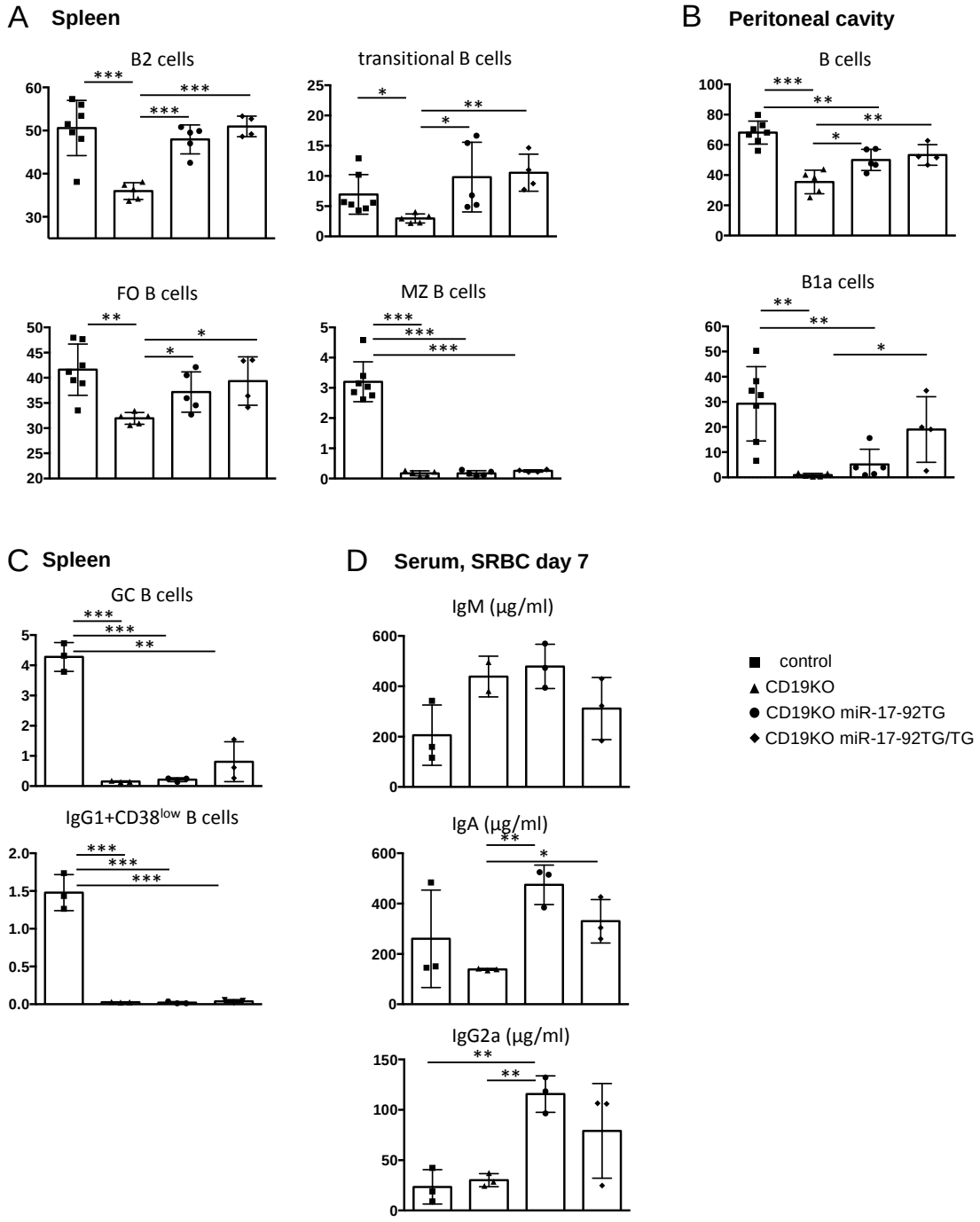

Supplementary figure 3 legend (related to figure 4)- Partial rescue of CD19KO B cells by miR-17-92 overexpression. (A) Graphs depict % cells amongst total splenocytes for transitional B cells ($B220^+AA4.1^+$), mature B2 B cells ($B220^+AA4.1^-$), follicular (FO) B cells ($B220^+AA4.1^-IgM^+CD1d^{low}$) and marginal zone (MZ) B cells ($B220^+AA4.1^-IgM^+CD1d^{high}$) (n=4-7). (B) Graphs depict % of peritoneal cavity derived B cells (IgM^+) and B1a B cells ($IgM^+B220^{+/low}CD5^+$) of the respective genotypes (n=4-7). (C) Graphs depict % of cells amongst total splenocytes for germinal center (GC) B cells ($B220^+CD38^{low}Fas^{high}$) and class switched $IgG1^+$ B cells ($B220^+CD38^{low}IgG1^+$)

on day 7 upon immunization with sheep red blood cells (SRBC). (D) Graph depicts Serum IgM (top), IgA (middle) and IgG2a (bottom) levels of the indicated genotypes on day 7 upon immunization with SRBC (n=2-3). Graphs depict mean values and SDs of the respective populations. Significance was calculated by the two-tailed student *t* test (*, $P<0.05$; **, $P<0.01$; ***, $P<0.001$).

Knockdown of CD19 modifies the PI3K/Akt/GSK3/c-Myc axis and increases BCR-mediated AICD.

We have first confirmed that PI3K regulates AICD. WEHI-231 cells were stimulated with anti-IgM antibodies in the absence or presence of the PI3K inhibitor LY294002. The PI3K inhibitor effectively suppressed Akt phosphorylation and enhanced the sensitivity of WEHI-231 cells to AICD upon BCR ligation, as apoptosis rates measured by PI were increased by 1.8-2 folds relative to the control untreated cells (supplementary figure 4 A and B). Also, purified splenic B cells treated with LY294002 exhibit reduced Akt phosphorylation as measured by flow cytometry ((supplementary figure 4C).

To look for the role of CD19 in regulating AICD, WEHI 231 cells were treated to knock-down CD19 using a shRNA approach ($CD19^{kd}$). Efficiency of CD19 knock-down is shown by western blot analysis (about 8 folds reduction, supplementary figure 4D) and by flow cytometry (about 10 fold reduction, MFI=208 in $CD19^{wt}$ relative to MFI=22 in $CD19^{kd}$, supplementary figure 4E), whereas expression levels of sIgM remained unchanged (supplementary figure 4E). The analysis for BCR-induced cell death revealed that $CD19^{kd}$ cells exhibited heighten sensitivity to AICD. Thus, the rate of apoptosis in $CD19^{kd}$ cells was higher by 1.7 folds relative to $CD19^{wt}$ cells after 16 hours, and increased up to 2 folds after 24 hours (supplementary figure 4, F and G). In contrast, no difference in apoptosis was found in response to ionomycin stimulation (supplementary figure 4H), suggesting that the increased AICD observed in $CD19^{kd}$ cells is the consequence of altered BCR signaling.

In WEHI-231 $CD19^{kd}$ cells, the impaired PI3K activity is evident by the reduced phosphorylation of Akt relative to $CD19^{wt}$ cells in response to BCR ligation (supplementary figure 4I). We further found that the phosphorylation and inactivation of GSK3 (α and β) in WEHI-231 $CD19^{kd}$ cells is reduced relative to that of control cells (supplementary figure 4J). In agreement with these findings, we demonstrate that the expression of c-Myc in WEHI-231 $CD19^{kd}$ is profoundly reduced and drops to background level more rapidly after BCR ligation (within 2 hours, figure 4K, top panel),

thereby explaining the increased AICD of these cells. However, the use of GSK3 inhibitor Bio-acetoxime sustained c-Myc expression following anti-IgM stimulation in both $CD19^{kd}$ and $CD19^{wt}$ cells (supplementary figure 4K, compare upper to lower panels).

Supplementary Figure 4

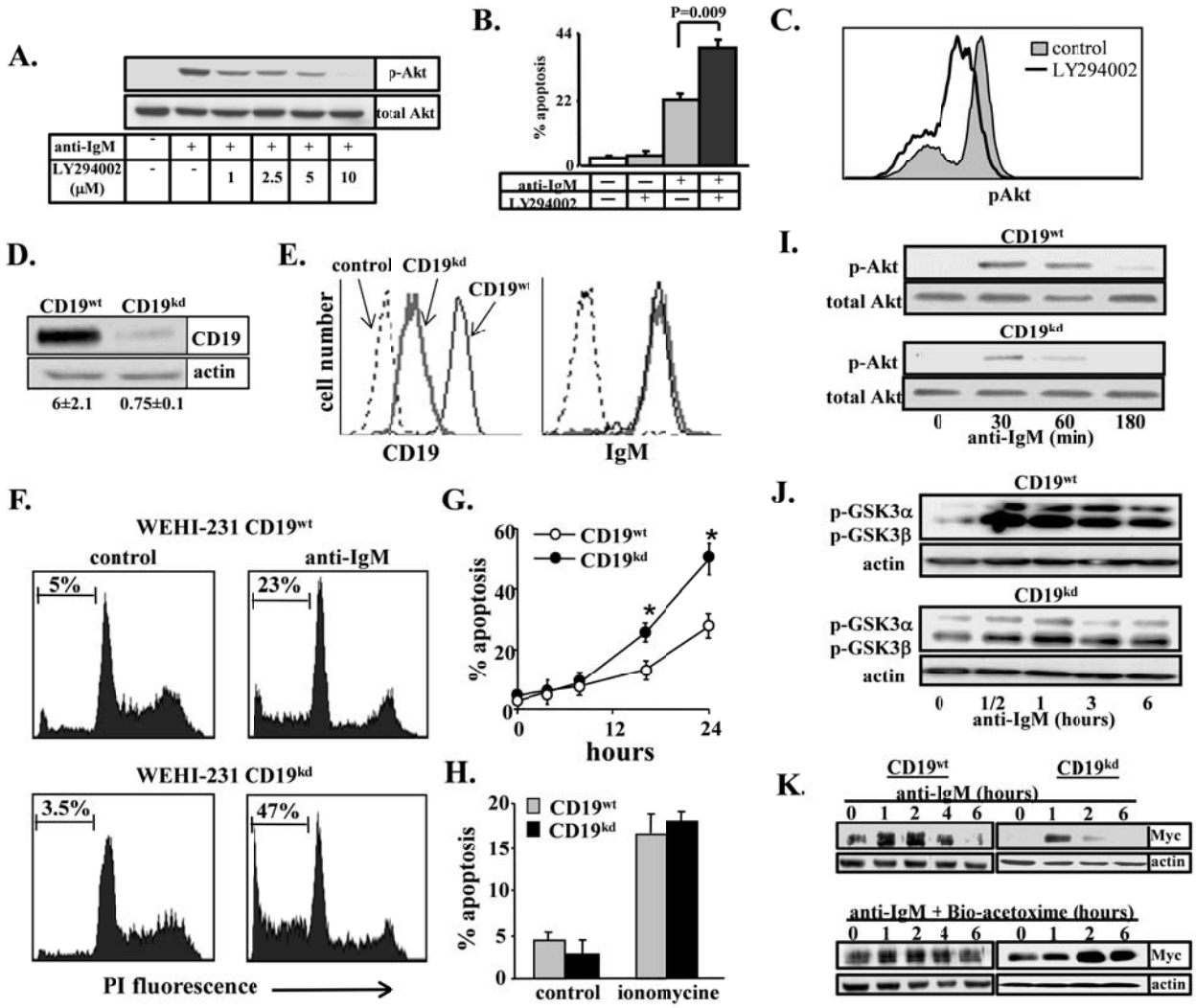

Supplementary figure 4 legend (related to figure 5)- (A) - WEHI-231 cells were treated with anti-IgM antibodies (10 μg/ml) in the presence of 0-10μM of PI3K inhibitor LY294002 for 30 minutes at 37°C. Cells were lysed and analyzed for Akt phosphorylation by Western blotting. (B) - WEHI-231 cells were treated with anti-IgM antibodies (10 μg/ml) in the absence or presence of 5μM LY294002 for 24 hours, stained with PI and analyzed for apoptosis by flow cytometry. The histograms indicate apoptosis rate for each treatment. (C) pAkt measured by flow cytometry in purified splenic B cells cultured for 5 min alone or with 5μM LY294002. (D-H) WEHI-231 cells

were infected with vectors encoding shRNA targeting CD19 ($CD19^{kd}$) or a control shRNA sequence ($CD19^{wt}$). (D) – Immunoblot analysis of CD19 protein expression in $CD19^{wt}$ and $CD19^{kd}$ cell lysates. Relative level of CD19 protein was determined by densitometry analysis (numbers at the bottom of each lane), where the CD19 band was quantified and normalized to that of the actin band. (E) –Flow cytometry for surface expression of CD19 and IgM. (F and G) – Cells were stimulated with anti-IgM (10 μg/ml) for different time intervals (0-24 hours), stained with PI and analyzed by flow cytometry for apoptosis. (F) - A representative PI analysis of apoptosis in cells stimulated for 24 hours. (G) – Kinetic measurement of apoptosis in cells that were stimulated with anti-IgM antibodies for 0-24 hours measured by PI. The results shown are from three experiments. An asterisk indicates statistical significant difference ($p<0.05$) (H) - Cells were stimulated with ionomycin (4μM) for 24 hours stained with PI and analyzed for apoptosis by FACS. (I-K) - WEHI-231 $CD19^{kd}$ and $CD19^{wt}$ cells were treated with anti-IgM (10μg/ml) for the indicated time points, lysed and analyzed for Akt phosphorylation (I), GSK3α and GSK3β phosphorylation (J). Cells were stimulated with anti-IgM (10μg/ml) for the indicated time points in the presence or absence of GSK3 inhibitor Bio-acetoxime (0.2μM). Cells were lysed to determine c-Myc protein expression by Western blotting (K).

Knockdown of CD19 increases AICD in apoptosis-resistant B lymphoma cells.

Since knockdown of CD19 increases susceptibility to AICD in WEHI-231 cells, we tested whether this experimental maneuver will render apoptosis-resistant B lymphoma cells more susceptible to AICD. The 38C-13 mouse B lymphoma cells are more resistant to AICD as anti-BCR ligation enhances apoptosis by only two folds (supplementary figure 5B). The knockdown of CD19 in these cells (supplementary figure 5A) significantly increased apoptosis rate by >12 folds (from 3.5% in unstimulated cells to 44% in cells stimulated with anti-IgM, supplementary figure 5B, bottom). Further biochemical analysis revealed that the knockdown of CD19 leads to an early drop of c-Myc expression in response to BCR ligation (supplementary figure 5C). Similarly, we found that knockdown of CD19 in the apoptosis-resistant human B lymphoma cells BJAB (supplementary figure 5E, top) significantly increased apoptosis rate by >7 folds (from 3.6% in unstimulated cells to 26% in cells stimulated with anti-IgM, supplementary figure 5E, bottom). Thus, resistance to AICD in B lymphoma cells can be prevailed by knockdown of CD19 expression.

Supplementary Figure 5

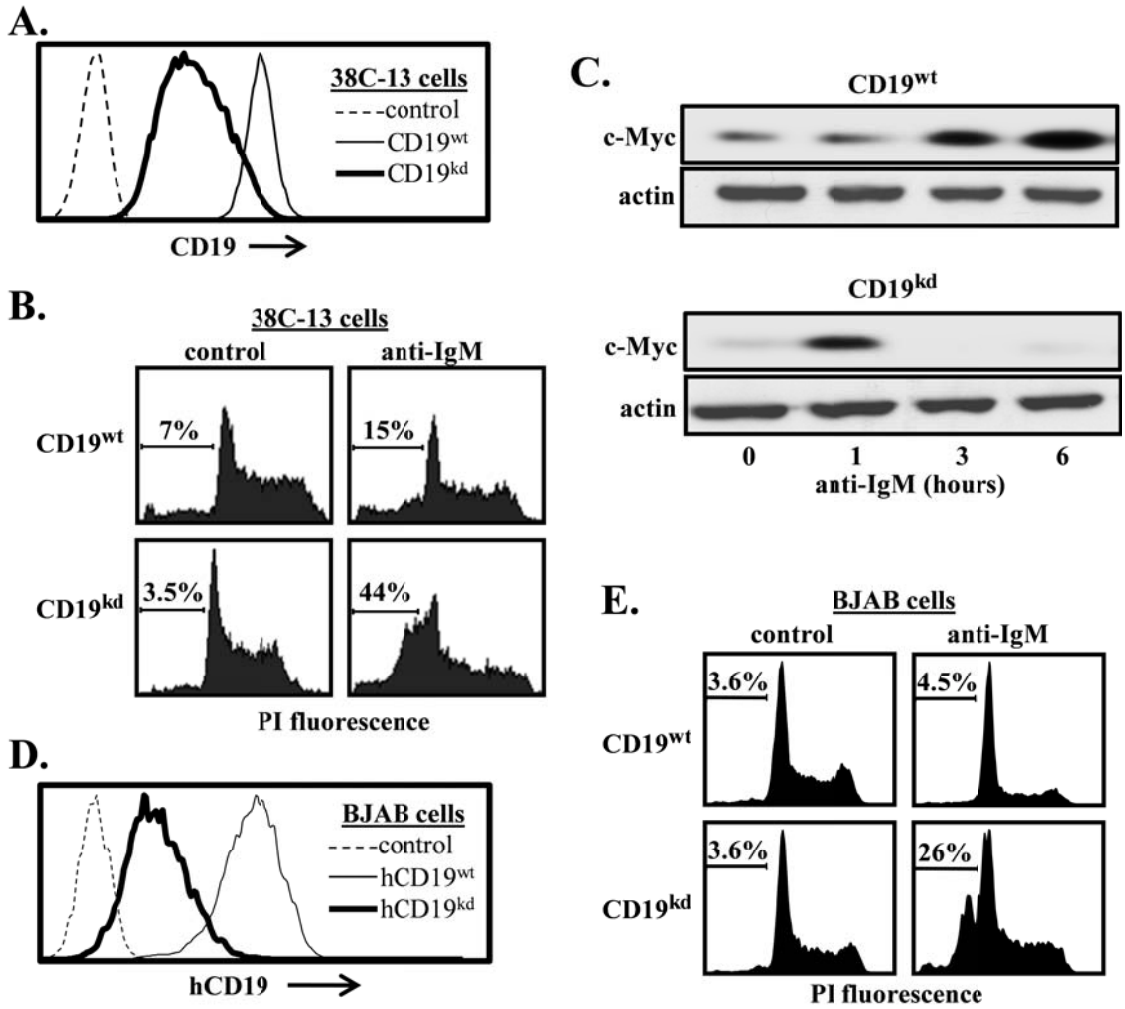

Supplementary figure 5 legend (related to figure 5)- The mouse B lymphoma 38C-13 were treated to knockdown CD19 using the viral vector encoding shRNA to mouse CD19. (A) –Flow cytometry for surface expression of CD19. (B) – Cells were stimulated with anti-IgM (10 μg/ml) for 24h stained with PI and analyzed by flow cytometry for apoptosis. (C) - Cells were stimulated with anti-IgM (10μg/ml) for the indicated time intervals and lysed to determine c-Myc protein expression by Western blotting.

The human B lymphoma BJAB were treated to knockdown CD19 using a viral vector encoding shRNA to human CD19. (D) –Flow cytometry for surface expression of CD19. (E) – Cells were stimulated with anti-IgM (10 μg/ml) for 24h stained with PI and analyzed by flow cytometry for apoptosis.

Over expression of CD19 enhances PI3K activity.

WEHI-231 cells were transfected with human CD19 (hCD19) to over express functional CD19 in these cells. Cells were sorted to hCD19+ and hCD19-. We found no difference in level of mouse CD19 expression between the two sorted cell populations (supplementary figure 6A). In response to BCR ligation we found increased phosphorylation of Akt, GSK3 and consequential increased expression of c-Myc in hCD19+ cells. This indicates that in hCD19+ cells PI3K activity is enhanced.

Supplementary Figure 6

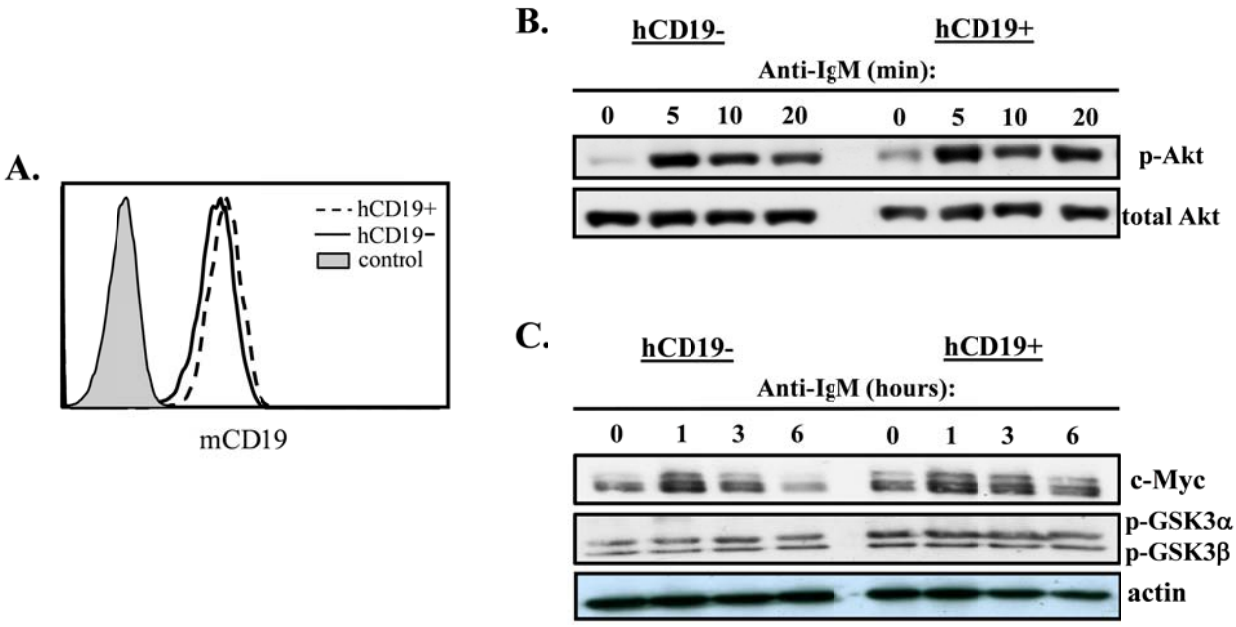

Supplementary figure 6 legend (related to figure 5)– WEHI 231 cells were transfected to express human CD19 (hCD19). After transfection, cells were sorted to hCD19+ and hCD19-. (A) Cells were stained for expression of mouse CD19 (mCD19) and analyzed by flow cytometry. Mean fluorescence intensity for mCD19 is shown for each sorted population. (B) - Cells were stimulated with anti-IgM (10µg/ml) for the indicated time points and lysed to determine phosphorylation of Akt by Western blotting. (C) - Cells were stimulated with anti-IgM (10µg/ml) for the indicated time points and lysed to determine c-Myc protein expression and phosphorylation of GSK3 by Western blotting.

Antisense c-Myc oligonucleotides (ASOs) suppresses expression of c-Myc.

To suppress c-Myc expression in B cells we used c-Myc antisense oligonucleotides (ASOs) as described (3). In response to anti-IgM stimulation we show that c-Myc expression is increased significantly whereas in the presence of c-Myc ASOs expression of c-Myc is suppressed (supplementary figure 7).

Supplementary Figure 7

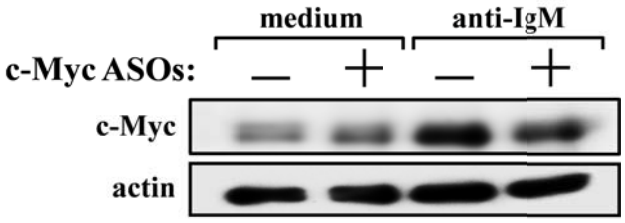

Supplementary figure 7 legend (related to figure 2)– Purified splenic B cells were cultured with c-Myc antisense oligonucleotides (ASOs) at 1μM for 8h. Cells were then stimulated with anti-IgM antibodies for 1h, lysed and analyzed for c-Myc expression by western blotting.

Methodology

Western blot analysis. Western blotting was performed as we have previously described (4). Briefly, cells were lysed in RIPA buffer containing complete protease inhibitor cocktail (Roche Diagnostics), 1mM sodium orthovanadate, 5mM sodium fluoride and 0.5mM phenylmethylsulfonyl fluoride. Proteins were separated by SDS-PAGE and transferred to polyvinylidene fluoride membrane (Millipore, Bedford, MA). Blots were probed with rabbit anti-phospho-Akt (Ser473) (Cat 4060), rabbit anti-Akt (Cat 9272), rabbit anti-phospho-GSK3α/β (Cat 9331), rabbit anti-Pten (Cat 9188), rabbit anti-CD19 (Cat 3574), rabbit anti-mouse c-Myc (Cat 5605) (all from Cell Signaling), mouse anti-actin (C4) (from MP biomediacls). To reveal bound Abs we used HRP conjugated secondary Abs. Blots were developed with ECL reagent (Pierce). To obtain semiquantitative estimates for total CD19, bands were quantified and densitometry analysis was performed using Tina 2.0 software (Raytest, Straubenhardt, Germany). Values were normalized to the respective control bands.

Flow cytometry. Generation of single-cell suspensions from mouse organs was performed by gentle homogenization through nylon mesh filters (70 μM; BD; spleen) or mechanic disruption of cell clusters by pipetting (peritoneal washes). Erythrocytes in spleens were lysed with ACK lysis buffer on ice before staining, and cell numbers determined using a hemocytometer (Neubauer) and trypan blue exclusion. Single cell suspensions for flow cytometry were stained with the following antibodies: αB220-BV785 (RA3-6B2), αCD19-BV605 (6D5), αCD93-APC (AA4.1), αCD38-APC (90) and αCD5-PE (53-7.3) αhCD19-APC (HIB19), αIgD-PE (11-26c.2a), αB220-PB (RA3-6B2), from BioLegend, αCD1d-PE (1B1) from eBioscience, αCD95-PeCy7 (Jo2) and αIgG1-PE (A85-1) from BD, αCD19-FITC (6D5) from Southern Biotechnology Association and goat α-mouse IgM, μ chain specific, from Jackson ImmunoResearch. Single-cell suspensions prepared from cells grown in BM cultures were stained with various fluorescently labeled antibodies to the indicated surface markers. In some experiments cells were stained with APC-Annexin V (cat 640920) from BioLegend according manufacturer instructions. In some experiments we conducted intracellular

stain using anti-phosphorylated Akt-PE (S473, clone D9E) from Cell Signaling. Data were acquired on LSRFortessa (BD Pharmingen) and analyzed using FlowJo software (Tree star inc).

Cell stimulations. For stimulations, 2-5 × 10^6 cells were resuspended in culture medium at 37ºC and stimulated with polyclonal goat anti mouse IgM antibodies (Southern Biotechnology Associates, Birmingham, AL) or with the F(ab')2 of goat anti-mouse IgM (Jackson ImmunoResearch) at 0.1-20 μg/ml or with ionomycine (4μM) (Sigma). In some of the experiments, we used the PI(3)K inhibitor LY294002 (1-20 μM) (Sigma) or the GSK3α/β inhibitor Bio-acetoxime (Tocris bioscience, Bristol UK) (0.2μM) or anti-sense c-Myc oligonucleotydes (1μM) (3). Stimulations were allowed to proceed for the indicated time intervals and cells were lysed for Western blot or for mRNA and microRNA analysis. In some experiments, immature B cells that were grown in IL-7-driven BM cultures (5) were sorted and stimulated with F(ab')2 of goat anti-mouse IgM for 12h and analyzed for apoptosis by flow cytometry.

Generation of viral vectors. To knockdown mouse CD19 expression, we transfected WEHI-231 cells or 38C-13 cells with pSUPER viral vector encoding mouse CD19 shRNA. Targeting shRNA sequence was cloned into hind III and bgl II sites of pSUPER retroviral expression vector using the following oligonucleotides:

Forward - 5'gatccccGACACACACACACTCATATttcaagagaATATGAGTGTGTGTGTGTCtttttggaaa-3'

Reverse - 5'agcttttccagcttttccaaaaaGACACACACACACTCATATtctcttgaaATATGAGTGTGTGTGTGTCgg g-3'

As a control we constructed a viral vector containing a non targeting sequence using the following oligonucleotides:

Forward - 5'gatccccTAGATGAAGGCACCTATTAttcaagagaTAATAGGTGCCTTCATCTAttttttggaaa-3'

Reverse-

5'agcttttccagcttttccaaaaaTAGATGAAGGCACCTATTAtctcttgaaTAATAGGTGCCTTCATCTAgg

g-3'

To knockdown human CD19 in BJAB cells we used shRNA lentiviral infection. To do so, five individual clones from MISSION™ shRNA Target Set NM_001770 were co-transfected with a lentivirus packaging plasmid into HEK 293T cells. The most effective sequence to knockdown hCD19 was used in the experiments detailed here (ccggtgggcattcttcatcttcaaactcgagtttgaagatgaagaatgcccatttttg).

To overexpress hCD19, the cloned human CD19 cDNA was purchased from ORIGENE (Rockville, MD, USA) and cloned into pIRES GFP, the hCD19-IRES fragment was excised from the pIRES and inserted into SIN18-pRLL-hEFIαp-EGFP-WRPE (6) to get the SIN18-pRLL-hEFIαp hCD19 IRES EGFP-WRPE vector (Prachel).

To overexpress the cluster miR17-92 in Wehi-231 cells we used MSCV-Puro-IRES-GFP (MSCVPIG) empty vector and MSCV-PIG with miR-17-92 (7). To suppress miR19b in WEHI-231 we used pMSCV-PIG-sp19 encoding a sponge system to miR19b as has been described (8)

To overexpress Pten in Wehi-231 cells we used an inducible Tet-on expression system as ectopic Pten overexpression was found to be cytotoxic. To do so, human Pten was obtained from (9) and cloned into P. Inducer GFP vector (10) and single GFP^{hi} clones were grown. Pten expression was induced upon induction with 1μg/ml doxycycline. To test for AICD, cells were co-treated with 1μg/ml doxycycline and with anti-IgM antibodies for 12h and analyzed for AICD. To knockdown Pten expression we used a viral vector encoding shPten (LENG.ShPten 1523, (11)). In some experiments, Wehi-231 cells were first infected with LENG.ShPten1523 vector and after selection the cells were infected with pMSCV-PIG-sp19 to generate cells where Pten is knockdown and miR19b is suppressed.

Viral Packaging and Infection. For retroviral infections, virus production and infection of cells were performed as we have described (12). Briefly, retroviral vectors were transfected into Phoenix cells

and following 48h at 37°C, viral-rich supernatant was collected and filtered with 0.45μm diameter pore filter. For infection, $1x10^6$ cells were resuspended in 1 ml of viral sup with 10 μg/ml polybrene (American Bioanalytical) and placed in 24-well plates. Next, cells were centrifuged at 140g for 60 min, resuspended in culture medium and incubated for 16h at 37°C. Cells were then transferred to petri dishes for additional 24h, followed by addition of puromycin (Sigma) at 3μg/ml for 14 days to select stably transfected clones.

For lentivirus Prachel hCD19 or MISSION™ shRNA Target Set NM_001770 were co-transfected into HEK 293T cells together with a lentivirus packaging plasmid. The resulting lentiviral particles were used for infection of BJAB cells.

Quantitative Real-Time PCR

Quantitative PCR analysis of mature miRNA was performed as has been described (13) and modified as follows. Briefly, RNA was extract by using Tri-Reagent (Sigma). All specimens of RNAs were polyadenylated with poly(A) polymerase (NEB). RNA was reverse-transcribed with Moloney murine leukemia virus reverse transcriptase (NEB) and 0.5μg poly(T) adaptor. DNA was amplified by Syber green mix (Tiangen) with specific miRNA primer and 3′ adaptor primer. U6 small nuclear RNA served as the endogenous reference gene. Reactions were performed on BioRad CFX connect Real-Time PCR.

Gene	Species	Primer-Forward	Primer-Reverse
U6 snRNA	Mouse/Human	GAC TAT CAT ATG CTT ACC GT	GCG AGC ACA GAA TTA ATA CGA C
MiR-29a	Mouse	TAG CAC CAT CTG AAA TCG GTT A	GCG AGC ACA GAA TTA ATA CGA C
MiR-150	Mouse	TCT CCC AAC CCT TGT ACC AGT G	GCG AGC ACA GAA TTA ATA CGA C
MiR19b-3p	Mouse/Human	TGT GCA AAT CCA TGC AAA ACT GA	GCG AGC ACA GAA TTA ATA CGA C
PTEN	Mouse	TGG ATT CGA CTT AGA CTT GAC CT	GCG GTG TCA TAA TGT CTC TCA G
GAPDH	Mouse	TGA AGC AGGCAT CTG AGG G	CGA AGG TGG AAG AGT GG AG
Pri-MiR19b	Mouse	GTCCTGTTATTGAGCACTGG	CCATACAGAGAAACACAGCA

Table1: Primers for qPCR

Gene Set Enrichment Analysis. Microarray data of B-cell lymphoma conditionally inactivated for MYC and overexpressing miR-17-92 and compared to wild type controls were obtained from Li et al. (14), GEO:GSE4475. Differentially expressed genes in each of the two conditions (Myc or mir-17-92 inactivation) were ranked by top-most absolute log-2 fold-change and thresholded based on

the overlap with the Li et al. p-value derived differentially expressed list, at 91% of genes (Extending coverage between fold-change and p-value to a full 100% yielded a list thousands of genes long). Based on this we also computed a list of shared Myc-mir-17-92 targets. The obtained lists of shared MYC and miR-17-92 and mir-17-92-only target genes was then profiled using GSEA against a set of 140 microarray expression profiles of B-cell lymphomas, obtained from GEO:GSE4475 and split into CD19 high versus low expression. Pten was later added to a copy of each test set, to examine its effect on enrichment. For statistical testing, data were permuted 1,000 times and the‘‘meandiv’’ normalization algorithm was applied.

1. Ahuja, A., J. Shupe, R. Dunn, M. Kashgarian, M. R. Kehry, and M. J. Shlomchik. 2007. Depletion of B cells in murine lupus: efficacy and resistance. *J Immunol* 179:3351-3361.
2. Norvell, A., and J. G. Monroe. 1996. Acquisition of surface IgD fails to protect from tolerance-induction. Both surface IgM- and surface IgD-mediated signals induce apoptosis of immature murine B lymphocytes. *J Immunol* 156:1328-1332.
3. Leider, N., and D. Melamed. 2003. Differential c-Myc responsiveness to B cell receptor ligation in B cell-negative selection. *J Immunol* 171:2446-2452.
4. Keren, Z., E. Diamant, O. Ostrovsky, E. Bengal, and D. Melamed. 2004. Modification of Ligand-independent B Cell Receptor Tonic Signals Activates Receptor Editing in Immature B Lymphocytes. *J Biol Chem* 279:13418-13424.
5. Melamed, D., J. A. Kench, K. Grabstein, A. Rolink, and D. Nemazee. 1997. A functional B cell receptor transgene allows efficient IL-7- independent maturation of B cell precursors. *J Immunol* 159:1233-1239.
6. Kafri, T., U. Blomer, D. A. Peterson, F. H. Gage, and I. M. Verma. 1997. Sustained expression of genes delivered directly into liver and muscle by lentiviral vectors. *Nat Genet* 17:314-317.
7. Mu, P., Y.-C. Han, D. Betel, E. Yao, M. Squatrito, P. Ogrodowski, E. de Stanchina, A. D'Andrea, C. Sander, and A. Ventura. 2009. Genetic dissection of the miR-17∼92 cluster of microRNAs in Myc-induced B-cell lymphomas. *Genes & Development* 23:2806-2811.
8. Kluiver, J., J. H. Gibcus, C. Hettinga, A. Adema, M. K. S. Richter, N. Halsema, I. Slezak-Prochazka, Y. Ding, B.-J. Kroesen, and A. van den Berg. 2012. Rapid Generation of MicroRNA Sponges for MicroRNA Inhibition. *PLoS ONE* 7:e29275.
9. Furnari, F. B., H. Lin, H.-J. S. Huang, and W. K. Cavenee. 1997. Growth suppression of glioma cells by PTEN requires a functional phosphatase catalytic domain. *Proceedings of the National Academy of Sciences* 94:12479-12484.
10. Meerbrey, K. L., G. Hu, J. D. Kessler, K. Roarty, M. Z. Li, J. E. Fang, J. I. Herschkowitz, A. E. Burrows, A. Ciccia, T. Sun, E. M. Schmitt, R. J. Bernardi, X. Fu, C. S. Bland, T. A. Cooper, R. Schiff, J. M. Rosen, T. F. Westbrook, and S. J. Elledge. 2011. The pINDUCER lentiviral toolkit for inducible RNA interference in vitro and in vivo. *Proc Natl Acad Sci USA* 108:3665-3670.
11. Fellmann, C., T. Hoffmann, V. Sridhar, B. Hopfgartner, M. Muhar, M. Roth, Dan Y. Lai, Inês A. M. Barbosa, Jung S. Kwon, Y. Guan, N. Sinha, and J. Zuber. 2013. An Optimized microRNA Backbone for Effective Single-Copy RNAi. *Cell Reports* 5:1704-1713.
12. Novak, R., E. Jacob, J. Haimovich, O. Avni, and D. Melamed. 2010. The MAPK/ERK and PI3K pathways additively coordinate the transcription of recombination-activating genes in B lineage cells. *J Immunol* 185:3239-3247.

13. Shi, R., and V. L. Chiang. 2005. Facile means for quantifying microRNA expression by real-time PCR. *Biotechniques* 39:519-525.
14. Li, Y., Peter S. Choi, Stephanie C. Casey, David L. Dill, and Dean W. Felsher. 2014. MYC through miR-17-92 Suppresses Specific Target Genes to Maintain Survival, Autonomous Proliferation, and a Neoplastic State. *Cancer Cell* 26:262-272.